ICES Report 04-29

DISCRETE COMPACTNESS FOR THE *hp* VERSION OF RECTANGULAR EDGE FINITE ELEMENTS

DANIELE BOFFI, MARTIN COSTABEL, MONIQUE DAUGE, AND LESZEK DEMKOWICZ

Abstract. In this paper we prove the discrete compactness property for the edge element approximation of Maxwell's eigenpairs on general *hp* adaptive rectangular meshes. Hanging nodes, yielding 1-irregular meshes, are covered, and the order of the used elements can vary from one rectangle to the other, thus allowing for a real *hp* adaptivity. As a consequence of our result, for the first time a rigorous proof of convergence for the p version of edge element approximation of Maxwell's eigenproblem is presented.

1. Introduction

In this paper we deal with the discrete compactness property of edge finite elements for the approximation of Maxwell's eigenvalues. This property has been well studied in the framework of the h version of edge finite elements where it is well known to hold true for a variety of edge finite elements on quite general two and three dimensional meshes (see the review papers [22, 13], the book [25], and the references therein, among which we recall in particular [23, 6, 3, 26, 4, 11, 9]), but has not been widely investigated for the p and *hp* version yet. On the other hand, electromagnetic devices very often involve complicated geometries, which in particular may not be smooth or convex. The analysis of the singularities arising from reentrant corners or edges and from material discontinuities (see [12, 14]) shows that such situations are to be handled with care. When using edge elements, one might want to locally adapt the meshsize h and the approximation order p, which can possibly vary from one element to the other within the same mesh. Such an *hp strategy* is an excellent way to get accurate results (an *exponential convergence* is expected and observed) when even severe singularities are present (see [29, 15] for examples of *hp* finite element implementations).

In [5], the analysis of the discrete compactness property for triangular *hp* finite elements has been tackled, but the proof of the main result relied on a conjectured L^2 estimate which had only been demonstrated numerically. Even for the pure p method, there is no result in this direction available in the literature. In [24] the p version of edge elements has been considered, but the proved results do not apply to eigenvalue approximations.

In this paper, we consider the two dimensional case of rectangular elements. A rigorous proof of the discrete compactness property is provided for edge elements of the first Nedelec family. Our hypotheses allow for a complete *hp* refinement, including the presence of hanging nodes. The pure p version of edge elements, being a subset of our setting, is naturally

Date: 16 September 2004.

1991 *Mathematics Subject Classification.* 65N30, 65N25, 78M10.

Key words and phrases. Maxwell equations, *hp* finite elements, discrete compactness, edge elements, eigenvalue approximation.

covered by our analysis. The same proof applies to mesh of quadrilaterals obtained by affine transformation from the reference square (i.e., parallelograms). The case of general quadrilateral meshes presents some issues (see [2]); the validity of the discrete compactness property for the p and hp versions of edge elements remains an open problem in this case.

Our presentation starts with the pure p method on a single square element, which is analyzed in Section 3 after the introduction of some preliminary notation in Section 2. We consider, in particular, full tensor polynomials (the second Nedelec family of edge elements, see [28]) and standard edge element of the first Nedelec family (see [27]). We show that standard edge elements provide convergent approximation, while the second Nedelec family presents several spurious eigenvalues (more precisely, discrete eigenvalues with wrong multiplicity). We then present in Section 4 the general hp theory which relies on an L^2 estimate which is proved thanks to the evaluation of an inf-sup constant on the reference element (Section 4.3). We make use of the hp edge element spaces presented in [29], which generalize the first family of Nedelec finite elements. In Section 5 we start an analysis of spectral properties of the "ABF" elements that have been introduced (see [2]) to improve the approximation properties of edge elements on non-affine quadrilaterals. Our analysis of the discrete eigenvalues on a square element suggests that these elements might provide a spectrally correct approximation.

2. Preliminary notions and notation

2.1. **Polynomial spaces on the reference square.** The square is defined as $\Sigma := I^2$ where I is the interval $(-1, 1)$. We denote the coordinates by $\mathbf{x} = (x, y)$. The outward unit normal vector on the boundary $\partial\Sigma$ is $\mathbf{n}$.

Everywhere p denotes an integer $p \geq 1$. The space of polynomials of degree $\leq p$ on I is denoted by $\mathbb{P}^p(I)$, its subspace of polynomials φ with zero traces, $\varphi(\pm 1) = 0$, is denoted by $\mathbb{P}^p_0(I)$.

On the square, let $\mathbb{Q}^{p,q}(\Sigma)$ be the space of polynomials of separate degrees p and q in x and y, respectively. This can be expressed as

$$\mathbb{Q}^{p,q}(\Sigma) = \mathbb{P}^p(I) \otimes \mathbb{P}^q(I).$$

Symbol $\mathbb{Q}^p$ will be used for isotropic spaces, $\mathbb{Q}^p = \mathbb{Q}^{p,p}$, and $\mathbb{Q}^p_0$ will denote the polynomials with zero traces, $\mathbb{Q}^p_0 = \mathbb{P}^p_0 \otimes \mathbb{P}^p_0$.

We will study in the following two families of polynomial spaces for the electric field $\mathbf{u} = (u_1, u_2)$ on the square Σ. We postpone to Section 5 the introduction and the investigation of a third family, namely the augmented ABF family [2].

2.1.1. *Full tensor product spaces:* $\mathbf{Q}^p(\Sigma)$ denotes the full space $\mathbb{Q}^p(\Sigma) \times \mathbb{Q}^p(\Sigma)$. This is the space of Lagrange nodal elements on the square and, with appropriate degrees of freedom, this forms also the *second Nedelec family* of edge elements.

We denote by $\mathbf{Q}^p_{\mathsf{N}}(\Sigma)$ its subspace of the fields $\mathbf{u}$ satisfying the perfect electric conductor boundary condition $\mathbf{u} \times \mathbf{n} = 0$ on $\partial\Sigma$. We have

$$\mathbf{Q}^p_{\mathsf{N}}(\Sigma) = \big[\mathbb{P}^p(I) \otimes \mathbb{P}^p_0(I)\big] \times \big[\mathbb{P}^p_0(I) \otimes \mathbb{P}^p(I)\big]. \tag{1}$$

2.1.2. *Classical edge elements:* $\mathbf{N}^p(\Sigma)$ denotes the space $\mathbb{Q}^{p-1,p}(\Sigma) \times \mathbb{Q}^{p,p-1}(\Sigma)$ which allows the commuting diagram property with the operator **grad** from the space of scalar polynomials $\mathbb{Q}^p(\Sigma)$. This edge element spaces are also known as *first Nedelec family* of edge elements. For simplicity, we shall refer to the spaces of this section as standard (Nedelec) edge elements. We denote by $\mathbf{N}^p_{\mathsf{N}}(\Sigma)$ the subspace of fields satisfying the electric boundary condition:

$$\mathbf{N}^p_{\mathsf{N}}(\Sigma) = \big[\mathbb{P}^{p-1}(I) \otimes \mathbb{P}^p_0(I)\big] \times \big[\mathbb{P}^p_0(I) \otimes \mathbb{P}^{p-1}(I)\big]. \tag{2}$$

2.2. **Maxwell spectrum in the square.** In Section 3 we shall describe in terms of 1D problems the Maxwell spectrum computed with the spaces $\mathbf{Q}^p_{\mathsf{N}}(\Sigma)$ and $\mathbf{N}^p_{\mathsf{N}}(\Sigma)$.

We first recall the definition of the standard continuous spaces associated with Maxwell equations on a domain Ω: $\mathbf{H}(\mathrm{curl}, \Omega)$ is the space of $L^2(\Omega)$ fields with curl in $L^2(\Omega)$, while $\mathbf{H}_0(\mathrm{curl}, \Omega)$ is the subspace of $\mathbf{H}(\mathrm{curl}, \Omega)$ with perfect electric boundary conditions; $\mathbf{H}(\mathrm{div}, \Omega)$ is the space of $L^2(\Omega)$ fields with divergence in $L^2(\Omega)$.

Let us describe the Maxwell spectrum in the continuous space

$$\mathbf{X}_{\mathsf{N}}(\Sigma) := \mathbf{H}_0(\mathrm{curl}, \Sigma) \cap \mathbf{H}(\mathrm{div}, \Sigma)\,,$$

i.e., the eigenpairs $(\lambda, \mathbf{u})$ with $\mathbf{u} \neq 0$ such that

$$\mathbf{u} \in \mathbf{X}_{\mathsf{N}}(\Sigma) : \quad \int_\Sigma \mathrm{curl}\,\mathbf{u}\ \mathrm{curl}\,\mathbf{v}\, d\mathbf{x} = \lambda \int_\Sigma \mathbf{u} \cdot \mathbf{v}\, d\mathbf{x}, \quad \forall \mathbf{v} \in \mathbf{X}_{\mathsf{N}}(\Sigma).$$

2.2.1. *The kernel:* for $\lambda = 0$, we have the whole space $\mathbf{grad}\, H^1_0(\Sigma)$ of kernel elements.

2.2.2. *The genuine Maxwell spectrum:* the whole non-zero spectrum corresponds to eigenvectors of the form $\mathbf{u} = \mathbf{curl}\,\varphi$ with φ non-constant eigenvector of the Neumann problem on Σ. Let $(\psi_j)_{j\geq 0}$ be the basis of the Neumann eigenvectors on the interval I, they are associated with the eigenvalues $j^2\pi^2/4$. Then, the Maxwell spectrum on Σ is

$$\lambda_{j,k} = (j^2 + k^2)\pi^2/4, \quad \mathbf{u}_{j,k}(x,y) = \big(\psi_j(x)\psi'_k(y), -\psi'_j(x)\psi_k(y)\big), \quad j + k \geq 1. \tag{3}$$

For comparison purposes, it is convenient to split the whole spectrum into the three following parts.

- **(a)** The kernel.
- **(b)** The non-zero Neumann eigenvalues $j^2\pi^2/4$ associated with the two eigenvectors
$$\big(0, -\psi'_j(x)\big) \quad \text{and} \quad \big(\psi'_j(y), 0\big).$$
- **(c)** The sum of two non-zero Neumann eigenvalues $(j^2 + k^2)\pi^2/4$ with the eigenvectors $\mathbf{u}_{j,k}$ (and $\mathbf{u}_{k,j}$ if $j \neq k$).

Remark 1. For all non-constant Neumann eigenvectors ψ_j (i.e., for $j \geq 1$), ψ'_j is a Dirichlet eigenvector associated with the eigenvalue $j^2\pi^2/4$. Let us denote $\varphi_j := -\psi'_j$. Then $(j^2\pi^2/4)\psi_j = -\psi''_j = \varphi'_j$, and we can see that eigenvectors associated with part **(c)** of the spectrum can be written as

$$\Big(\frac{1}{j^2}\,\varphi'_j(x)\varphi_k(y), -\frac{1}{k^2}\,\varphi_j(x)\varphi'_k(y)\Big). \tag{4}$$

3. Approximation of Maxwell's spectrum in a square by the p method

In this section we characterize explicitly the Maxwell spectrum on the square computed with the full polynomial space $\mathbf{Q}^p_{\mathsf{N}}(\Sigma)$ and with the Nedelec edge element space $\mathbf{N}^p_{\mathsf{N}}(\Sigma)$.

In contrast with (3), where the 1D generators are the *Neumann* eigenvectors on the interval, at the discrete level we will show that the 1D generators are the *Dirichlet* discrete eigenvectors: for $p \geq 2$, we consider the eigenpairs (λ, β) with $\beta \neq 0$ such that

$$\beta \in \mathbb{P}^p_0(I): \quad \int_I \beta' w'\, dx = \lambda \int_I \beta w\, dx, \quad \forall w \in \mathbb{P}^p_0(I). \tag{5}$$

The dimension of $\mathbb{P}^p_0(I)$ is $p-1$; for $j = 1, \ldots, p-1$, let $\big(\lambda_j^{[p]}, \beta_j^{[p]}\big)$ be an eigenpair basis of (5) satisfying

$$\lambda_1^{[p]} < \lambda_2^{[p]} < \ldots < \lambda_{p-1}^{[p]}.$$

For each j, $\lambda_j^{[p]}$ tends exponentially to $j^2\pi^2/4$ as $p \to \infty$.

We are going to describe the Maxwell spectrum in $\mathbf{Q}^p_{\mathsf{N}}(\Sigma)$, i.e., the eigenpairs $(\lambda, \mathbf{u})$ such that

$$\mathbf{u} \in \mathbf{Q}^p_{\mathsf{N}}(\Sigma): \quad \int_\Sigma \operatorname{curl} \mathbf{u}\, \operatorname{curl} \mathbf{v}\, d\mathbf{x} = \lambda \int_\Sigma \mathbf{u} \cdot \mathbf{v}\, d\mathbf{x}, \quad \forall \mathbf{v} \in \mathbf{Q}^p_{\mathsf{N}}(\Sigma). \tag{6}$$

Theorem 1. *The whole Maxwell spectrum* (6) *in* $\mathbf{Q}^p_{\mathsf{N}}(\Sigma)$ *can be split into four parts.*

- **(a)** *The kernel:* $\lambda = 0$ *and* $\mathbf{u} \in \mathbf{grad}(\mathbb{P}^p_0 \otimes \mathbb{P}^p_0)$.
- **(b)** *The Dirichlet discrete eigenvalues* $\lambda_j^{[p]}$ *associated with the two eigenvectors*

$$\big(0, -\beta_j^{[p]}(x)\big) \quad \text{and} \quad \big(\beta_j^{[p]}(y), 0\big), \quad j = 1, \ldots, p-1. \tag{7}$$

- **(c)** *The sum of two Dirichlet discrete eigenvalues* $\lambda_j^{[p]} + \lambda_k^{[p]}$ *with the eigenvectors*

$$\big(\lambda_j^{[p]} \beta_k^{[p]\prime}(x) \beta_j^{[p]}(y), -\lambda_k^{[p]} \beta_k^{[p]}(x) \beta_j^{[p]\prime}(y)\big), \quad 1 \leq j, k \leq p-1. \tag{8}$$

- **(d)** *The Dirichlet discrete eigenvalues* $\lambda_j^{[p]}$ *associated with two* spurious *eigenvectors*

$$\big(0, -\beta_j^{[p]}(x) L_p(y)\big) \quad \text{and} \quad \big(L_p(x) \beta_j^{[p]}(y), 0\big), \tag{9}$$

where L_p *denotes the Legendre polynomial of degree* p.

Remark 2. Note that formula (4) transforms into $\big(j^2 \varphi_k'(x) \varphi_j(y), -k^2 \varphi_k(x) \varphi_j'(y)\big)$ by swapping j and k and multiplying by $j^2 k^2$. The similarity with formula (8) is now obvious.

Remark 3. The previous theorem shows that the space $\mathbf{Q}^p_{\mathsf{N}}(\Sigma)$ is not suited for the computation of Maxwell's eigenvalues. Indeed, the discrete eigenvalues described in part **(d)** are redundant, providing a wrong multiplicity to the correct eigenvalues described in part **(b)**. Moreover, the discrete eigenvectors of part **(d)** do not approximate any physical eigenfunction.

Proof. Let us first check the dimensions of the spaces described in the four above cases:

- **(a)** $(p-1)^2$
- **(b)** $2(p-1)$
- **(c)** $(p-1)^2$
- **(d)** $2(p-1)$.

The sum is $2(p-1)(p+1)$, which is the dimension of $\mathbf{Q}^p_{\mathsf{N}}(\Sigma)$ (see (1)).

It remains to check that the proposed pairs are eigenpairs of (6).

Case (a). The scalar polynomial space $\mathbb{P}^p_0 \otimes \mathbb{P}^p_0$ is contained in $H^1_0(\Sigma)$, therefore all elements of $\mathbf{grad}(\mathbb{P}^p_0 \otimes \mathbb{P}^p_0)$ belong to the kernel.

For the remaining part of the proof, since p is fixed, let us drop the exponent $[p]$ in the notation of the discrete 1D Dirichlet eigenpairs. By integration by parts we note that the discrete eigenpairs (λ_j, β_j) satisfy

$$\int_I (\beta_j'' + \lambda_j \beta_j)\, w\, dx = 0, \quad \forall w \in \mathbb{P}^p_0(I). \tag{10}$$

On the other hand, again by integration by parts, we obtain that $(\lambda, \mathbf{u})$ is an eigenpair in $\mathbf{Q}^p_{\mathsf{N}}(\Sigma)$, if and only if

$$\mathbf{u} \in \mathbf{Q}^p_{\mathsf{N}}(\Sigma) : \quad \int_\Sigma (\mathbf{curl}\,\mathrm{curl}\,\mathbf{u} - \lambda \mathbf{u}) \cdot \mathbf{v}\, d\mathbf{x} = 0, \quad \forall \mathbf{v} \in \mathbf{Q}^p_{\mathsf{N}}(\Sigma). \tag{11}$$

It is clear that all proposed eigenvectors in **(b)**, **(c)** and **(d)** belong to $\mathbf{Q}^p_{\mathsf{N}}(\Sigma)$. It remains to compute $\mathbf{curl}\,\mathrm{curl}\,\mathbf{u} - \lambda\mathbf{u}$ in each case and to check (11).

Case (b). For $\lambda = \lambda_j$ and $\mathbf{u} = \big(0, -\beta_j(x)\big)$, the two components of $\mathbf{curl}\,\mathrm{curl}\,\mathbf{u} - \lambda\mathbf{u}$ are

$$0 \quad \text{and} \quad \beta_j''(x) + \lambda_j \beta_j(x).$$

Then relation (10) yields (11), and the same argument applies to the other vector $\big(\beta_j(y), 0\big)$.

Case (c). For $\lambda = \lambda_j + \lambda_k$ and $\mathbf{u}$ given by (8), we have

$$\mathrm{curl}\,\mathbf{u} = (\lambda_j + \lambda_k)\beta_k'(x)\beta_j'(y)$$

and the two components of $\mathbf{curl}\,\mathrm{curl}\,\mathbf{u} - \lambda\mathbf{u}$ are

$$\begin{aligned} &-(\lambda_j + \lambda_k)\beta_k'(x)\beta_j''(y) - (\lambda_j + \lambda_k)\lambda_j \beta_k'(x)\beta_j(y) \\ &+(\lambda_j + \lambda_k)\beta_k''(x)\beta_j'(y) + (\lambda_j + \lambda_k)\lambda_k \beta_k(x)\beta_j'(y) \end{aligned}$$

which can be written as

$$\begin{aligned} &-(\lambda_j + \lambda_k)\beta_k'(x)\big\{\beta_j''(y) + \lambda_j\beta_j(y)\big\} \\ &(\lambda_j + \lambda_k)\beta_j'(y)\big\{\beta_k''(x) + \lambda_k\beta_k(x)\big\}. \end{aligned}$$

Then relation (10) yields (11).

Case (d). For $\lambda = \lambda_j$ and $\mathbf{u} = \big(0, -\beta_j(x)L_p(y)\big)$, the two components of $\mathbf{curl}\,\mathrm{curl}\,\mathbf{u} - \lambda\mathbf{u}$ are

$$-\beta_j'(x)L_p'(y) \quad \text{and} \quad \beta_j''(x)L_p(y) + \lambda_j\beta_j(x)L_p(y).$$

The second component is orthogonal to any element of $\mathbb{P}^p_0(I) \otimes \mathbb{P}^p(I)$ (see (1) and (10)). It remains to check that the first component is orthogonal to $\mathbb{P}^p(I) \otimes \mathbb{P}^p_0(I)$, i.e.,

$$\int_\Sigma v_j'(x)L_p'(y)w(x)v(y)\, dxdy = 0, \quad \forall w \in \mathbb{P}^p(I), \quad \forall v \in \mathbb{P}^p_0(I). \tag{12}$$

It it sufficient to prove that $\int_I L_p'(y)v(y)\, dy = 0$ for all $v \in \mathbb{P}^p_0(I)$: such a v is given by $(1-y^2)\varphi(y)$ with $\varphi \in \mathbb{P}^{p-2}(I)$. Since the polynomials L_k' are orthogonal on I with respect to the measure $(1-y^2)\, dy$ and since the degree of L_j' is $j-1$, we obtain that

$$\int_I L_p'(y)\varphi(y)(1-y^2)\, dy = 0, \quad \forall \varphi \in \mathbb{P}^{p-2}(I),$$

hence (12). □

The next theorem characterizes the Maxwell spectrum in $\mathbf{N}^p_{\mathsf{N}}(\Sigma)$, i.e., the eigenpairs $(\lambda, \mathbf{u})$ such that

$$\mathbf{u} \in \mathbf{N}^p_{\mathsf{N}}(\Sigma) : \quad \int_\Sigma \operatorname{curl} \mathbf{u} \operatorname{curl} \mathbf{v}\, d\mathbf{x} = \lambda \int_\Sigma \mathbf{u} \cdot \mathbf{v}\, d\mathbf{x}, \quad \forall \mathbf{v} \in \mathbf{N}^p_{\mathsf{N}}(\Sigma). \tag{13}$$

Theorem 2. *The three first parts* **(a)**, **(b)**, *and* **(c)** *of the discrete spectrum described in Theorem 1 are the whole discrete Maxwell spectrum computed by the edge element space* $\mathbf{N}^p_{\mathsf{N}}(\Sigma)$.

Proof. We can see that the eigenvectors of parts **(a)**, **(b)**, and **(c)** all belong to the smaller space $\mathbf{N}^p_{\mathsf{N}}(\Sigma)$. Therefore they are also eigenvectors in this space. We see that the sum of the dimensions of the corresponding eigenspaces is $(p-1)^2 + 2(p-1) + (p-1)^2$, which is equal to $2(p-1)p$, the dimension of $\mathbf{N}^p_{\mathsf{N}}(\Sigma)$ (see (2)). □

The conclusion arising from Theorems 1 and 2 is that the space $\mathbf{N}^p_{\mathsf{N}}(\Sigma)$ is to be preferred with respect to $\mathbf{Q}^p_{\mathsf{N}}(\Sigma)$ for the computation of Maxwell's eigenpairs. Indeed, the latter space does not provide correct approximation of the spectrum (see Remark 3).

4. Approximation of Maxwell's spectrum by *hp* rectangular finite elements

In this section we extend the results about the space $\mathbf{N}^p_{\mathsf{N}}(\Sigma)$ to the more involved situation of *hp* refinements, which provides realistic applications to polygonal domains. The structure of this section is as follows. First of all, we define the finite element spaces we are dealing with, and make precise the assumptions on the mesh. Then, after establishing an L^2 stability result (see Section 4.3), we prove the discrete compactness property which implies the convergence of eigenvalues/eigenvectors. Our proof clearly implies that the discrete compactness property holds true also for the pure p method on a conforming rectangular mesh (i.e., without hanging node) with the standard edge elements of the first Nedelec family.

4.1. De Rham diagram for a variable order quad element.

Let $\Sigma = I \times I$ be the master square element. A feature of edge elements is their embedding in a *commuting de Rham diagram* of type (14) relating two exact sequences of spaces, on both continuous and discrete levels. We refer to [22, 9] for a systematic description of the standard discrete de Rham diagram of any degree, where the interpolation operators are based on nodal values, edge and volume moments. In view of the construction *hp* finite elements, another class of commuting de Rham diagram has been introduced [18], relying on the so called *projection-based interpolants*, which allow variable orders on distinct elements of the same mesh, while preserving the commuting property.

We start by introducing this latter version of the de Rham diagram, involving discrete spaces and interpolation operators on Σ, according to

$$\begin{array}{ccccccccc}
\mathbb{R} & \longrightarrow & H^{1+\varepsilon}(\Sigma) & \xrightarrow{\mathbf{grad}} & \mathbf{H}^{\varepsilon}(\Sigma) \cap \mathbf{H}(\operatorname{curl}, \Sigma) & \xrightarrow{\operatorname{curl}} & L^2(\Sigma) & \longrightarrow & \mathbf{0} \\
\Big\downarrow id & & \Big\downarrow \Pi & & \Big\downarrow \Pi^{\operatorname{curl}} & & \Big\downarrow \mathrm{P} & & \\
\mathbb{R} & \longrightarrow & \mathbb{Q}^{p|\,p_e}(\Sigma) & \xrightarrow{\mathbf{grad}} & \mathbf{N}^{p|\,p_e-1}(\Sigma) & \xrightarrow{\operatorname{curl}} & \mathbb{Q}^{p-1}(\Sigma) & \longrightarrow & \mathbf{0}
\end{array} \tag{14}$$

Index p specifies the order in both variables which, for the sake of simplicity of this presentation, we assume to be identical, $\mathbb{Q}^p(\Sigma) = \mathbb{Q}^{p,p}(\Sigma) = \mathbb{P}^p(I) \otimes \mathbb{P}^p(I)$, and with every edge e of the master element, we associate the corresponding order p_e, $e = 1, \ldots, 4$ (with standard, counterclockwise enumeration of edges) that satisfies the condition:

$$p_e \leq p, \;\; e = 1, \ldots, 4. \tag{15}$$

The polynomial spaces present in the diagram are defined as follows.

- $\mathbb{Q}^{p|\,p_e}(\Sigma)$ - the subspace of $\mathbb{Q}^p(\Sigma)$, consisting of polynomials whose traces on edges e reduce to (possibly lower) order p_e, $e = 1, \ldots, 4$.
- $\mathbf{N}^{p|\,p_e}(\Sigma)$ - the subspace of $\mathbf{N}^p(\Sigma)$, *cf* §2.1.2, of vector-valued polynomials with traces of their tangential components on edges e of (possibly lower) order p_e:

$$\mathbf{N}^{p|\,p_e}(\Sigma) = \{\mathbf{u} \in \mathbf{N}^p(\Sigma) : u_t|_e := (\mathbf{n} \times \mathbf{u})|_e \in \mathbb{P}^{p_e}(e), \;\forall e\}, \tag{16}$$

  where $\mathbf{n}$ is the outward unit normal vector.

In particular, $\mathbb{Q}^{p|\,-1}$ provides an alternative notation for the subspace $\mathbb{Q}^p_0$ of polynomials vanishing on the boundary of the element, and $\mathbf{N}^{p|\,-1} = \mathbf{N}^p_{\mathsf{N}}$ stands for the subspace of vector-valued polynomials from the first Nedelec family whose tangential component traces on the boundary are equal to zero. The assumption that edge orders p_e should not exceed corresponding components of order p, is realized in practice by implementing the *minimum rule* that sets an edge order p_e to the minimum of orders p corresponding to the adjacent elements.

4.1.1. **H^1-conforming projection-based interpolation.** Let $\mathbb{P}^p_0(I)$ denote the space of polynomials of degree $\leq p$, defined on the interval $I = (-1, 1)$ with zero traces at the endpoints. Let $\phi_1(x) = (1 - x)/2$, $\phi_2(x) = (x + 1)/2$ be the standard 1D linear shape functions. Space $\mathbb{Q}^p_{p_e}(\Sigma)$ admits a natural decomposition into vertex bilinear shape functions, edge bubbles and element bubbles

$$\begin{aligned} \mathbb{Q}^{p|\,p_e}(\Sigma) = &\left\{\mathbb{P}^1(I) \otimes \mathbb{P}^1(I)\right\} \oplus \\ &\left\{\mathbb{P}^{p_1}_0(I) \otimes \mathbb{R}\phi_1) \oplus (\mathbb{R}\phi_2 \otimes \mathbb{P}^{p_2}_0(I)) \oplus (\mathbb{P}^{p_3}_0(I) \otimes \mathbb{R}\phi_2) \oplus (\mathbb{R}\phi_1 \otimes \mathbb{P}^{p_4}_0(I)\right\} \oplus \\ &\left\{\mathbb{P}^p_0(I) \otimes \mathbb{P}^p_0(I)\right\}. \end{aligned} \tag{17}$$

We will alternatively speak of edge bubbles for functions defined on a particular edge (and zero at its ends) or for their extensions to the whole element (and zero on the other edges). The linear extensions are natural but not essential in the forthcoming discussion. For a particular edge, the corresponding edge bubbles must vanish on the remaining edges and must "live" in the FE space. Similarly, the shape function for a vertex node must vanish at the remaining vertices and it must be in the FE space; the fact that it is constructed using bilinear functions, is secondary.

Given a function $u \in H^{1+\varepsilon}(\Sigma)$, we define its interpolant $u_p = \Pi u$, as a sum of three contributions,

$$u_p = u_1 + \underbrace{\sum_e u_{2,e,p}}_{u_{2,p}} + u_{3,p}\,. \tag{18}$$

Interpolation at vertices. Vertex interpolant u_1 interpolates function u at vertices,

$$u_1(a) = u(a) \quad \text{for each vertex } a.$$

The simplest choice of an extension of the vertex values is provided by the bilinear function but the ultimate value of the interpolant is independent of the choice of the extension as long as the extension "lives" in the FE space.

Projection on edges. We subtract the vertex interpolant u_1 from u and project the difference $u - u_1$, over each edge e, onto the space of edge bubbles,

$$|u - u_1 - u_{2,e,p}|_{1/2,e} \to \min .$$

The projection is done in an $H^{1/2}(e)$ seminorm, and it is equivalent to the solution of a small linear system (an edge Dirichlet problem),

$$\begin{aligned} &\textit{Find edge bubble } \ u_{2,e,p} \in \mathbb{P}_0^{p_e}(e) \ \textit{ such that} \\ &(u - u_1 - u_{2,e,p}\,, \phi)_{1/2,e} = 0, \quad \textit{for each edge bubble } \phi \in \mathbb{P}_0^{p_e}(e), \end{aligned}$$

where $(\cdot,\cdot)_{1/2,e}$ denotes the inner product corresponding to edge seminorm $|\cdot|_{1/2,e}$

Projection on the element. We extend each edge bubble $u_{2,e}$ to the whole element. Again, the most natural extension is provided by the element shape functions and corresponds to decomposition (18). We subtract then the total edge interpolant $u_2 = \sum_e u_{2,e}$ from the difference $u - u_1$ and project the resulting difference on the element bubbles,

$$|u - u_1 - u_{2,p} - u_{3,p}|_{1,\Sigma} \to \min .$$

Again, the projection is equivalent to a local Dirichlet problem on the element,

$$\begin{aligned} &\textit{Find element bubble } \ u_{3,p} \in \mathbb{Q}_0^{p}(\Sigma) \ \textit{ such that} \\ &(u - u_1 - u_{2,p} - u_{3,p}\,, \phi)_{1,\Sigma} = 0, \quad \textit{for each element bubble } \phi \in \mathbb{Q}_0^{p}(\Sigma), \end{aligned}$$

where $(\cdot,\cdot)_{1,\Sigma}$ denotes the H_0^1- inner product.

The interpolation is thus equivalent to the solution of a sequence of local (approximate) Dirichlet problems. We first interpolate at the vertices, and then, with the vertex values providing Dirichlet conditions, solve the edge Dirichlet problems. Finally, we use the vertex and edge interpolants to set up the Dirichlet boundary conditions and solve the final Dirichlet problem on the whole element. Remember that it does not matter in which way we construct lifts of the approximate Dirichlet data, the ultimate interpolant is unique. In each of the three steps, we determine a part of the interpolant corresponding to the decomposition (17).

4.1.2. **$\mathbf{H}$(curl)-conforming projection-based interpolation.** A similar decomposition into edge functions and element bubbles can be constructed for the space $\mathbf{N}^{p|\,p_e-1}(\Sigma)$,

$$\begin{aligned} \mathbf{N}^{p|\,p_e-1}(\Sigma) = \Big\{ &\big[(\mathbb{P}^{p_1-1}(I) \otimes \mathbb{R}\phi_1) \times \{0\}\big] \oplus \big[\{0\} \times (\mathbb{R}\phi_2 \otimes \mathbb{P}^{p_2-1}(I))\big] \oplus \\ &\big[(\mathbb{P}^{p_3-1}(I) \otimes \mathbb{R}\phi_2) \times \{0\}\big] \oplus \big[\{0\} \times (\mathbb{R}\phi_1 \otimes \mathbb{P}^{p_4-1}(I))\big] \Big\} \oplus \\ &\Big\{ \big[(\mathbb{P}^{p-1} \otimes \mathbb{P}_0^{p})(\Sigma) \times \{0\}\big] \oplus \big[\{0\} \times (\mathbb{P}_0^{p} \otimes \mathbb{P}^{p-1})(\Sigma)\big] \Big\}. \end{aligned} \tag{19}$$

Given a vector-valued function $\mathbf{u} \in \mathbf{H}^{\varepsilon}(\mathrm{curl}, \Sigma)$, we define its interpolant $\mathbf{u}_p = \Pi^{\mathrm{curl}}\mathbf{u}$ as a sum of two contributions,

$$\mathbf{u}_p = \underbrace{\sum_e \mathbf{u}_{2,e,p}}_{\mathbf{u}_{2,p}} + \mathbf{u}_{3,p}.$$

Edge projections. For each edge e, let $v_t = \mathbf{n} \times \mathbf{v}$ denote the (scalar-valued) tangential component of a field $\mathbf{v}$ on e. We project the tangential component u_t of function $\mathbf{u}$ onto the scalar edge functions,

$$\|u_t - u_{2,e,p,t}\|_{-1/2,e} \to \min.$$

Here the norm $\|\cdot\|_{-1/2,e}$ denotes the norm in the dual space

$$H^{-1/2}(e) = (H^{1/2}_{00}(e))'.$$

We define then the vector edge function $\mathbf{u}_{2,e,p}$ as the tangent vector field on e such that $u_{2,e,p,t} = \mathbf{n} \times \mathbf{u}_{2,e,p}$. The projection problem is equivalent to the variational problem

Find the tangential component $u_{2,e,p,t} \in \mathbb{P}^{p_e-1}(e)$ *of the edge function* $\mathbf{u}_{2,e,p}$ *s. t.*

$(u_t - u_{2,e,p,t}, \phi)_{-1/2,e} = 0$, *for each edge function* $\phi \in \mathbb{P}^{p_e-1}(e)$,

with $(\cdot,\cdot)_{-1/2,e}$ denoting the inner product corresponding to norm $\|\cdot\|_{-1/2,e}$. Notice that for a constant function ϕ, the inner product reduces to L^2-product, and the equation above incorporates in particular the edge average condition

$$\int_e (u_t - u_{2,e,p,t})\, ds = 0.$$

Element projection. We extend each individual edge function $\mathbf{u}_{2,e,p}$ to the whole element using the edge shape functions according to the splitting (19), sum it up, $\mathbf{u}_{2,p} = \sum_e \mathbf{u}_{2,e,p}$, and subtract the difference from function $\mathbf{u}$. We solve then a local projection problem,

$$\|\,\mathrm{curl}(\mathbf{u} - \mathbf{u}_{2,p} - \mathbf{u}_{3,p})\|_{0,\Sigma} \to \min,$$

subjected to the additional constraint,

$$(\mathbf{u} - \mathbf{u}_{2,p} - \mathbf{u}_{3,p}, \mathbf{grad}\,\phi) = 0, \quad \text{for each element scalar bubble } \phi.$$

The constrained projection problem is equivalent to a Dirichlet mixed problem
Find element bubble $\mathbf{u}_{3,p}$ and Lagrange multiplier ψ such that

$$\text{(20)} \quad \begin{cases} (\mathrm{curl}(\mathbf{u} - \mathbf{u}_{2,p} - \mathbf{u}_{3,p}), \mathrm{curl}\,\mathbf{v}) + (\mathbf{grad}\,\psi, \mathbf{v}) = 0 & \text{for every element vector bubble } \mathbf{v} \\ (\mathbf{u} - \mathbf{u}_{2,p} - \mathbf{u}_{3,p}, \mathbf{grad}\,\phi) = 0 & \text{for every element scalar bubble } \phi. \end{cases}$$

Here, the Lagrange multiplier ψ lives in the space of scalar bubbles. Since $\mathbf{grad}\,\psi$ is a vector bubble, the multiplier is identically equal zero and, for this reason, it is sometimes called the *hidden variable*.

Remark 4. In [16], the edge contributions $\mathbf{u}_{2,e,p}$ were split into the Whitney interpolant with constant tangential component, and a higher order edge bubble. Also, the choice of "edge" norms in the presentation above is consistent with the latest 3D results, see [17], and it is slightly different from those used in [16].

Finally P is the L^2 projection from $L^2(\Sigma)$ onto $\mathbb{Q}^{p-1}(\Sigma)$. With this, we have:

Theorem 3. *If the edge seminorm* $|u|_{1/2,e}$ *is selected in such a way that*

$$|u|_{1/2,e} = \left\| \frac{\partial u}{\partial s} \right\|_{-1/2,e}$$

then the de Rham diagram (14) *commutes.*

Proof. The proof follows exactly the same lines as in [18] and we will not reproduce it here. Notice only that the condition above is justified as the tangential derivative defines a continuous map from $H^{1/2}(e)$ into $H^{-1/2}(e)$ (see [21, p. 31]). □

4.2. **De Rham diagram for *hp* meshes.** In this section we consider a polygonal domain Ω with sides parallel to the axes, covered by rectangular meshes aligned along the same axes. Of course, by a global affine transformation, our result generalizes to the situation of non perpendicular axes.

If we fix a conforming mesh (i.e., such that the intersection of any two distinct elements $\overline{K}$ is either a vertex or a full edge), and consider on each K the mapped spaces $\mathbb{Q}^{p|\,p}(K)$, $\mathbf{N}^{p|\,p-1}(K)$, and $\mathbb{Q}^{p-1}(K)$ with the same p, we can define on the whole domain Ω the corresponding H^1-, $\mathbf{H}$(curl)-, and L^2-conforming discrete spaces Q_p, $\mathbf{X}_p$ and S_p, and the projection-based interpolation is done element by element. The elements are said *unconstrained* in this case. Then it is clear that the commutativity properties (14) of the projection-based interpolation operators are still valid on the whole domain Ω. Besides, we note that in this case the discrete spaces coincide with those of the standard p-extension of the edge elements [27, 24].

The adaptation to *hp* meshes containing local refinements, therefore hanging nodes, and variable degrees is by no means obvious.

For the sake of simplicity of the presentation, we shall restrict ourselves to 1-irregular *hp* meshes corresponding to isotropic refinements only, and consisting of square elements. Beginning with a standard regular mesh consisting of square elements of the same size, we allow for breaking each element into four elements with the restriction that an element cannot share an edge with more than two small neighbors - the classical "two to one" rule. In other words, the *generation level* for two neighboring elements cannot differ by more than one. The order of elements can be modified locally, element by element, with the *minimum rule* being enforced - the order for an edge is set to the minimum of orders for all adjacent elements. Finally, since for meshes with hanging nodes the projections cannot be done on an element level - the resulting interpolants will no longer be conforming, the global conformity is maintained by means of the *constrained approximation*, see [29, 15].

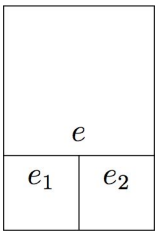

FIGURE 1. Constrained approximation

The situation is illustrated in Fig.1. For a function u defined on "big" edge e, the corresponding "big edge" interpolant is a polynomial defined on the whole edge, whereas the

interpolants determined on the small edges e_1, e_2 result in a piecewise interpolant that, in general, is different.

A natural idea is to utilize the constrained approximation concepts. First do the projections on the big edges and, then, define the corresponding small edges interpolants by enforcing the global conformity requirements. The resulting interpolants will be indeed globally conforming, but we loose then the commutativity properties. This can be seen by considering the lowest order elements. The last space in the diagram reduces then to piecewise constants and the commutativity property requires that

$$\int_{\partial K} (u_{p,t} - u_t)\, ds = \int_K \mathrm{curl}(\mathbf{u}_p - \mathbf{u})\, d\mathbf{x} = 0,$$

for each element K in the mesh. For regular meshes, the condition follows from the edge averaging. In presence of hanging nodes, however, the condition may not be satisfied. Going back to the situation illustrated in Fig. 1, enforcing the averaging condition on "big" edge e *does not imply* the same condition for the restrictions of the original function and its projection on the small edge e_1. Consequently, the condition above is violated for the small element, and the commutativity fails.

A remedy to the problem is to perform the interpolation on groups of elements. The whole mesh is split into *polygonal patches* consisting of single elements or *element clusters* (of minimum size) in such a way that all vertices of the polygonal patches are unconstrained. The decomposition is illustrated with the classical example of the L-shaped domain and h-refinements aimed at resolving the corner singularity shown in Fig 2.

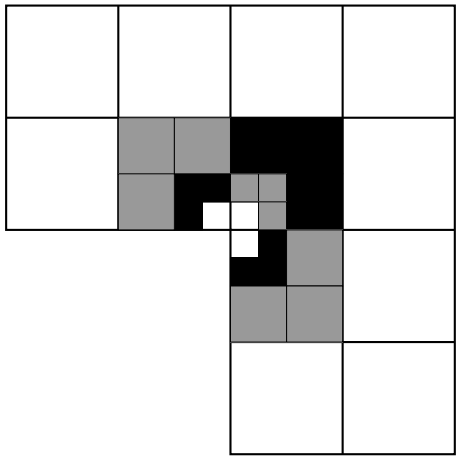

FIGURE 2. Decomposition of an 1-irregular mesh into clusters

All clusters in this example coincide with either a single element (the white elements) or three elements forming an L-shaped patch (such clusters are indicated in the picture with a grey or black shading). In general, the 1-irregularity rule limits the number of possible cluster shapes to four cases only: clusters of a single, two, three or four small elements. Our convention is to call patch, denoted by P, the union of the cluster elements K together with the interior edges. In our example, the L-shaped patches are the union of three squares and two interior edges, see Fig 3. Such patches have six distinct (exterior) edges. Edges of a

patch always coincide with either a single element edge or two "small" edges adjacent to a big one.

FIGURE 3. L-shaped cluster and patch

The space $\mathbb{Q}^{p|\,p_e}(P)$ on the patch is the subspace of continuous functions on P, which are $\mathbb{Q}^p$ on each element K of the cluster, and whose restriction on e belongs to $\mathbb{Q}^{p_e}(e)$ for each edge of the patch. The space $\mathbf{N}^{p|\,p_e-1}(P)$ is defined correspondingly as the subspace of $\mathbf{H}(\mathrm{curl})$ fields on P, which are in $\mathbf{N}^p$ on each element K, and whose tangential restriction on e belongs to $\mathbb{Q}^{p_e}(e)$.

The definition of projection-based interpolation extends now naturally to the patch P: We only list the main steps. The vertices are the corners of P and we check that there exists a continuous piecewise bilinear vertex interpolant $u_1 \in \mathbb{Q}^{1|\,1}(P)$. The edge bubbles $u_{2,e,p}$ are related with patch edges (and no more with element edges) and are polynomial on the whole patch edge. These bubbles can be extended inside P as elements of $\mathbb{Q}^{p|\,p_e}(P)$. The patch bubbles $u_{3,p}$ are the functions in the FE space $\mathbb{Q}^{p|\,p_e}(P)$ with zero traces on the patch boundary ∂P.

Similarly we define the edge functions $\mathbf{u}_{2,e,p}$ as vector polynomials on the whole patch edge, tangential to the edge. They can be extended in $\mathbf{N}^{p|\,p_e-1}(P)$. The patch bubbles $\mathbf{u}_{3,p}$ are the elements of $\mathbb{Q}^{p|\,p_e}(P)$ with zero tangential traces on the patch boundary ∂P. The patch bubbles are, therefore, no longer polynomials but *piecewise polynomials* only.

Thus, by the same procedure as before we define the projection operators

$$\Pi = \Pi_P, \quad \Pi^{\mathrm{curl}} = \Pi^{\mathrm{curl}}_P \quad \text{and} \quad \mathrm{P} = \mathrm{P}_P \tag{21}$$

and obtain a commutative scheme like (14).

Once the interpolation is done on the patches, we regain both the global conformity and commutativity of the interpolation operators on the whole hp mesh:

$$\begin{array}{ccccccccc}
\mathbb{R} & \longrightarrow & H^{1+\varepsilon}(\Omega) & \xrightarrow{\mathbf{grad}} & \mathbf{H}^{\varepsilon}(\Omega)\cap\mathbf{H}(\mathrm{curl},\Omega) & \xrightarrow{\mathrm{curl}} & L^2(\Omega) & \longrightarrow & \mathbf{0} \\
\big\downarrow id & & \big\downarrow \Pi & & \big\downarrow \Pi^{\mathrm{curl}} & & \big\downarrow \mathrm{P} & & \\
\mathbb{R} & \longrightarrow & Q_{hp} & \xrightarrow{\mathbf{grad}} & \mathbf{X}_{hp} & \xrightarrow{\mathrm{curl}} & S_{hp} & \longrightarrow & \mathbf{0}
\end{array}$$

Here Q_{hp}, $\mathbf{X}_{hp}$, S_{hp} denote FE spaces defined on the common domain Ω, corresponding to the H^1-, $\mathbf{H}(\mathrm{curl})$-, and L^2-conforming discretizations, done patch by patch.

4.3. **A stability result in L^2.** We begin by recalling the inclusion of polynomial spaces,

$$\mathbb{Q}^p_0(\Sigma) \xrightarrow{\mathbf{grad}} \mathbf{N}^p_{\mathsf{N}}(\Sigma).$$

Here,

$$\begin{aligned}\mathbb{Q}_0^p(\Sigma) &= \mathbb{P}_0^p(I)\otimes\mathbb{P}_0^p(I)\\ \mathbf{N}_{\mathsf{N}}^p(\Sigma) &= [\mathbb{P}^{p-1}(I)\otimes\mathbb{P}_0^p(I)]\times[\mathbb{P}_0^p(I)\otimes\mathbb{P}^{p-1}(I)].\end{aligned}$$

In this section, we will omit the mention of Σ and I for the spaces $\mathbb{Q}^p$, $\mathbf{N}^p$, and $\mathbb{P}^p$, respectively. We shall denote the L^2-norm on I or Σ, by $\|\cdot\|$, with the corresponding L^2-product denoted by $(\cdot,\cdot)$. We hope that the similarity of the latter with the notation for vector components will not lead to confusion.

Theorem 4. *The following stability condition holds:*

$$\inf_{\mathbf{q}\in\mathbf{N}_{\mathsf{N}}^p}\ \sup_{\mathbf{s}\in\mathbf{grad}\,\mathbb{Q}_0^p\oplus\mathbf{curl}\,\mathrm{curl}\,\mathbf{N}_{\mathsf{N}}^p}\frac{(\mathbf{q},\mathbf{s})}{\|\mathbf{q}\|\,\|\mathbf{s}\|}\ =\ C_p, \tag{22}$$

where

$$C_p=\left(\frac{2(2p+1)}{(p+1)(p+2)}\right)^{1/2}=O(p^{-1/2}). \tag{23}$$

The proof of Theorem 4 relies on two lemmas.

Lemma 5. *Let $a_i>0$, $b_i>0$, $i=1,\dots,n$. Then for any real $v_1,\dots,v_n$*

$$\sup_{u_1,\dots,u_n}\frac{|\sum_{i=1}^n a_iu_iv_i|}{(\sum_{i=1}^n b_iu_i^2)^{1/2}}=\left(\sum_{i=1}^n\frac{a_i^2}{b_i}v_i^2\right)^{1/2}.$$

Proof. Use Schwartz inequality for the discrete l^2 product and the representation,

$$\sum_{i=1}^n a_iu_iv_i=\sum_{i=1}^n\frac{a_i}{b_i^{1/2}}v_i\,b_i^{1/2}u_i.$$

□

We recall that (λ_i,β_i), $i=1,\dots,p-1$, denote the discrete eigenpairs of the 1D Laplace operator defined in equation (5) (we omit the exponent $[p]$ for simplicity). The eigenvectors are normalized to satisfy $(\beta_i,\beta_j)=\delta_{ij}$.

Lemma 6. *The following inequality holds.*

$$\left(\sum_{i=1}^{p-1}\lambda_i^2v_i^2\right)^{1/2}\ge C_p\|\sum_{i=1}^{p-1}v_i\beta_i''\|,\quad\forall\mathbf{v}=(v_1,\dots,v_{p-1})\in\mathbb{R}^{p-1},$$

where C_p is defined in (23).

Proof. It was proved in [5] that the constant

$$C_p\ =\ \inf_{u\,\in\,\mathbb{P}_0^p}\ \sup_{f\,\in\,\mathbb{P}^{p-2}}\frac{(u,f)}{\|u\|\|f\|}\ =\ \inf_{u\,\in\,\mathbb{P}_0^p}\ \sup_{v\,\in\,\mathbb{P}_0^p}\frac{(u,v'')}{\|u\|\|v''\|}\ =\ \inf_{u\,\in\,\mathbb{P}_0^p}\ \sup_{v\,\in\,\mathbb{P}_0^p}\frac{(u',v')}{\|u\|\|v''\|}$$

is given by formula (23). Consequently,

$$\sup_{u\,\in\,\mathbb{P}_0^p}\frac{(u',v')}{\|u\|}\geq C_p\|v''\|,\quad \forall v\in\mathbb{P}_0^p.$$

If we now define

$$u=\sum_{i=1}^{p-1}u_i\beta_i,\quad v=\sum_{i=1}^{p-1}v_i\beta_i,$$

then

$$(u',v')=\sum_{i=1}^{p-1}\lambda_i u_i v_i\qquad\text{and}\qquad \|u\|=\left(\sum_{i=1}^{p-1}u_i^2\right)^{1/2}.$$

Apply Lemma 5 to finish the proof. □

Proof of Theorem 4.
Step 1: let α_i, $i=0,\dots,p-1$ be a basis for $\mathbb{P}^{p-1}$ defined as follows

$$\alpha_i=\begin{cases}1/\sqrt{2} & i=0\\ \beta_i' & i=1,\dots,p-1.\end{cases}$$

Polynomials α_i are orthogonal and satisfy

$$\|\alpha_0\|^2=1,\quad \|\alpha_i\|^2=\lambda_i,\ i=1,\dots,p-1.$$

Any element $\mathbf{q}\in\mathbf{N}_{\mathsf{N}}^p$ can be represented in the form,

$$\mathbf{q}=\left(\sum_{i=0}^{p-1}\sum_{j=1}^{p-1}q_{1,ij}\alpha_i\beta_j,\sum_{i=1}^{p-1}\sum_{j=0}^{p-1}q_{2,ij}\beta_i\alpha_j\right).\tag{24}$$

Here and in what follows, we assume that in a tensor product $\alpha\beta$, the first function is always a function of x, and the second is a function of y, i.e., $\alpha\beta=\alpha(x)\beta(y)$.

A direct calculation shows that,

$$\begin{aligned}\mathbf{curl}\,\mathrm{curl}\,\mathbf{q}&=\left(\sum_{i=1}^{p-1}\sum_{j=0}^{p-1}q_{2,ij}\beta_i'\alpha_j'-\sum_{i=0}^{p-1}\sum_{j=1}^{p-1}q_{1,ij}\alpha_i\beta_j'',-\sum_{i=1}^{p-1}\sum_{j=0}^{p-1}q_{2,ij}\beta_i''\alpha_j+\sum_{i=0}^{p-1}\sum_{j=1}^{p-1}q_{1,ij}\alpha_i'\beta_j'\right)\\&=\left(\sum_{i=1}^{p-1}\sum_{j=1}^{p-1}q_{2,ij}\beta_i'\beta_j''-\sum_{i=0}^{p-1}\sum_{j=1}^{p-1}q_{1,ij}\alpha_i\beta_j'',-\sum_{i=1}^{p-1}\sum_{j=0}^{p-1}q_{2,ij}\beta_i''\alpha_j+\sum_{i=1}^{p-1}\sum_{j=1}^{p-1}q_{1,ij}\beta_i''\beta_j'\right)\\&=\left(-\sum_{j=1}^{p-1}q_{1,0j}\alpha_0\beta_j''+\sum_{i=1}^{p-1}\sum_{j=1}^{p-1}(q_{2,ij}-q_{1,ij})\beta_i'\beta_j'',-\sum_{i=1}^{p-1}q_{2,i0}\beta_i''\alpha_0-\sum_{i=1}^{p-1}\sum_{j=1}^{p-1}(q_{2,ij}-q_{1,ij})\beta_i''\beta_j'\right).\end{aligned}$$

Hence, any element $\mathbf{s}\in\mathbf{curl}\,\mathrm{curl}\,\mathbf{N}_{\mathsf{N}}^p$ can be represented in the form,

$$\mathbf{s}=\left(\sum_{j=1}^{p-1}s_{0j}\alpha_0\beta_j''+\sum_{i=1}^{p-1}\sum_{j=1}^{p-1}s_{ij}\beta_i'\beta_j'',\sum_{i=1}^{p-1}s_{i0}\beta_i''\alpha_0-\sum_{i=1}^{p-1}\sum_{j=1}^{p-1}s_{ij}\beta_i''\beta_j'\right).$$

Let $\mathbf{q}\in\mathbf{N}_{\mathsf{N}}^p$ be discrete divergence free, i.e.,

$$(\mathbf{q},\mathbf{grad}\,w)=0,\quad\forall w\in\mathbb{Q}_0^p.$$

Selecting $w = \beta_k\beta_l$, $k,l = 1,\dots,p-1$, we conclude that coefficients $q_{1,ij}, q_{2,ij}$ in representation (24) must satisfy the identity

$$q_{1,kl}\lambda_k + q_{2,kl}\lambda_l = 0.$$

This leads to the following formulas for the norm of a discrete divergence free vector, and the L^2-product of such a vector with $\mathbf{s} \in \mathbf{curl}\,\mathrm{curl}\,\mathbf{N}^p_{\mathsf{N}}$

$$\|\mathbf{q}\|^2 = \sum_{j=1}^{p-1} q_{1,0j}^2 + \sum_{i=1}^{p-1} q_{2.i0}^2 + \sum_{i=1}^{p-1}\sum_{j=1}^{p-1}\left(\frac{\lambda_i^2}{\lambda_j} + \lambda_i\right) q_{1,ij}^2$$

$$(\mathbf{q},\mathbf{s}) = -\sum_{j=1}^{p-1} q_{1,0j}s_{0j}\lambda_j - \sum_{i=1}^{p-1} q_{2,i0}s_{i0}\lambda_i - \sum_{i=1}^{p-1}\sum_{j=1}^{p-1} q_{1,ij}s_{ij}(\lambda_i\lambda_j + \lambda_i^2).$$

Applying Lemma 5 we get,

$$\sup_{\substack{\mathbf{q}\in\mathbf{N}^p_{\mathsf{N}}\\ (\mathbf{q},\mathbf{grad}\,w)=0,\ \forall w\in\mathbb{Q}^p_0}} \frac{(\mathbf{q},\mathbf{s})}{\|\mathbf{q}\|} = \sum_{j=1}^{p-1}\lambda_j^2 s_{0j}^2 + \sum_{i=1}^{p-1}\lambda_i^2 s_{i0}^2 + \sum_{i=1}^{p-1}\sum_{j=1}^{p-1}(\lambda_i^2\lambda_j + \lambda_i\lambda_j^2)s_{ij}^2.$$

Finally, the norm of $\mathbf{s} \in \mathbf{curl}\,\mathrm{curl}\,\mathbf{N}^p_{\mathsf{N}}$ can be represented in the form,

$$\|\mathbf{s}\|^2 = \left\|\sum_{j=1}^{p-1} s_{0j}\beta_j''\right\|^2 + \left\|\sum_{i=1}^{p-1} s_{i0}\beta_i''\right\|^2 + \sum_{i=1}^{p-1}\lambda_i\left\|\sum_{j=1}^{p-1} s_{ij}\beta_j''\right\|^2 + \sum_{j=1}^{p-1}\lambda_j\left\|\sum_{i=1}^{p-1} s_{ij}\beta_i''\right\|^2.$$

By Lemma 6 we have,

$$\sum_{j=1}^{p-1}\lambda_j^2 s_{0j}^2 \ge C_p^2\left\|\sum_{j=1}^{p-1} s_{0j}\beta_j''\right\|^2$$

$$\sum_{i=1}^{p-1}\lambda_i^2 s_{i0}^2 \ge C_p^2\left\|\sum_{i=1}^{p-1} s_{i0}\beta_i''\right\|^2$$

$$\lambda_i\sum_{j=1}^{p-1}\lambda_j^2 s_{ij}^2 \ge \lambda_i C_p^2\left\|\sum_{j=1}^{p-1} s_{ij}\beta_j''\right\|^2$$

$$\lambda_j\sum_{i=1}^{p-1}\lambda_i^2 s_{ij}^2 \ge \lambda_j C_p^2\left\|\sum_{i=1}^{p-1} s_{ij}\beta_i''\right\|^2.$$

Summing up all the inequalities, we get,

$$\sup_{\substack{\mathbf{q}\in\mathbf{N}^p_{\mathsf{N}}\\ (\mathbf{q},\mathbf{grad}\,w)=0,\ \forall w\in\mathbb{Q}^p_0}} \frac{(\mathbf{q},\mathbf{s})}{\|\mathbf{q}\|} \ge C_p\|\mathbf{s}\|,$$

or, equivalently, using the equality of inf-sup constants for a bilinear form and its adjoint,

$$\inf_{\substack{\mathbf{q}\in\mathbf{N}^p_{\mathsf{N}}\\ (\mathbf{q},\mathbf{grad}\,w)=0,\ \forall w\in\mathbb{Q}^p_0}} \sup_{\mathbf{s}\in\mathbf{curl}\,\mathrm{curl}\,\mathbf{N}^p_{\mathsf{N}}} \frac{(\mathbf{q},\mathbf{s})}{\|\mathbf{q}\|\|\mathbf{s}\|} \ge C_p. \tag{25}$$

Step 2: use discrete Helmholtz decomposition,

$$\mathbf{q} = \mathbf{q}_0 + \mathbf{grad}\,\phi, \quad (\mathbf{q}_0, \mathbf{grad}\,w) = 0 \ \forall w \in \mathbb{Q}_0^p, \quad \phi \in \mathbb{Q}_0^p.$$

to extend inequality (25) to arbitrary $\mathbf{q} \in \mathbf{N}_{\mathsf{N}}^p$ and $\mathbf{s} \in \mathbf{grad}\,\mathbb{Q}_0^p \oplus \mathbf{curl}\,\mathrm{curl}\,\mathbf{N}_{\mathsf{N}}^p$.

Step 3: The *equality* in (22) follows, e.g., from the fact that for $\mathbf{q}$ coinciding with eigenvectors from part **(b)** of the spectrum (see (7)), the two-dimensional inf-sup condition reduces to its one-dimensional counterpart. □

The consequence of Theorem 4 is the following L^2 stability result in p-version:

Theorem 7. *Let $\mathbf{u}_3 \in \mathbf{H}^\varepsilon(\Sigma) \cap \mathbf{H}_0(\mathrm{curl}, \Sigma)$ be a divergence free bubble function on Σ. Let $\mathbf{u}_{3,p}$ be the projection $\Pi^{\mathrm{curl}}\mathbf{u}_3$. Then $\mathbf{u}_{3,p}$ is discrete divergence free and there holds*

$$\|\mathbf{u}_3 - \mathbf{u}_{3,p}\|_{0,\Sigma} \leq Cp^{1/2} \inf_{\mathbf{q}_p \in \mathbf{N}_{\mathsf{N}}^p} \|\mathbf{u}_3 - \mathbf{q}_p\|_{0,\Sigma}. \tag{26}$$

Proof. Let $\mathbf{q}_p$ be any element of $\mathbf{N}_{\mathsf{N}}^p$. Since

$$(\Pi^{\mathrm{curl}}\mathbf{u}_3, \mathbf{grad}\,\mathbf{q}_p) = (\mathbf{u}_3, \Pi^{\mathrm{curl}}\,\mathbf{grad}\,\mathbf{q}_p) = (\mathbf{u}_3, \mathbf{grad}\,\Pi\mathbf{q}_p),$$

we obtain that $\mathbf{u}_{3,p}$ is discrete divergence-free.

By Theorem 4, there exists $\mathbf{s} \in \mathbf{grad}\,\mathbb{Q}_0^p \oplus \mathbf{curl}\,\mathrm{curl}\,\mathbf{N}_{\mathsf{N}}^p$ so that

$$C_p\|\mathbf{u}_{3,p} - \mathbf{q}_p\|\,\|\mathbf{s}\| \leq (\mathbf{u}_{3,p} - \mathbf{q}_p, \mathbf{s}).$$

Any $\mathbf{s} \in \mathbf{grad}\,\mathbb{Q}_0^p \oplus \mathbf{curl}\,\mathrm{curl}\,\mathbf{N}_{\mathsf{N}}^p$ being orthogonal to $\mathbf{u}_3 - \mathbf{u}_{3,p}$ we get

$$C_p\|\mathbf{u}_{3,p} - \mathbf{q}_p\|\,\|\mathbf{s}\| \leq (\mathbf{u}_3 - \mathbf{q}_p, \mathbf{s}) \leq \|\mathbf{u}_3 - \mathbf{q}_p\|\,\|\mathbf{s}\|.$$

By the triangle inequality we deduce (26). □

The best approximation error in the L^2 norm by polynomials in $\mathbf{N}_{\mathsf{N}}^p$ behaves as p^{-1} for fields in H^1 satisfying the boundary conditions of $\mathbf{H}_0(\mathrm{curl})$:

Lemma 8. *Let $\mathbf{u}_3 \in \mathbf{H}^1(\Sigma) \cap \mathbf{H}_0(\mathrm{curl}, \Sigma)$ be a general bubble function on Σ. There exists $\mathbf{q}_p \in \mathbf{N}_{\mathsf{N}}^p(\Sigma)$ such that*

$$\|\mathbf{u}_3 - \mathbf{q}_p\|_{0,\Sigma} \leq Cp^{-1}\|\mathbf{u}_3\|_{1,\Sigma}. \tag{27}$$

Proof. Let u_x and u_y be the two components of $\mathbf{u}_3$. We note that u_x belongs to $L^2(I, H_0^1(I)) \cap H^1(I, L^2(I))$. We take as interpolant for u_x the function $\pi_x^{p-1,0} \otimes \pi_y^{p,1}(u_x)$ where $\pi^{p,0}$ and $\pi^{p,1}$ are the 1D standard projection operators used in spectral and p methods: $\pi^{p,0}$ is the L^2 orthogonal projection on $\mathbb{P}^p(I)$ and $\pi^{p,1}$ is defined as

$$\pi^{p,1}(u)(t) = \int_{-1}^{t} \pi^{p-1,0}(u')(s)\,ds.$$

Both $\pi^{p,0}$ and $\pi^{p,1}$ satisfy the L^2-H^1 error estimate with a factor p^{-1}, see [30, Ch.3] for instance. Moreover $\pi^{p,0}$ is stable in L^2 and $\pi^{p,1}$ in H^1. The proof of the estimate for $\|u_x - \pi_x^{p-1,0} \otimes \pi_y^{p,1}(u_x)\|_{0,\Sigma}$ then follows. The situation for the second component is similar. □

4.4. **Discrete compactness.** In this section we prove the discrete compactness property for edge finite elements on 1-irregular *hp* square meshes. The discrete compactness property, stated in Theorem 11, is known to be sufficient and in a sense necessary for the good approximation of eigenvalues/eigenvectors (see [22, 4, 11, 26], for instance).

For our proof we need L^2 estimates for $\mathbf{u}-\Pi^{\mathrm{curl}}\mathbf{u}$ for divergence free fields $\mathbf{u}$ on any unconstrained element K (Lemma 9) or any patch P (Lemma 10).

Lemma 9. *Let K be an unconstrained square element of size $h=h_K$, and let p be the minimum among p_K and $\{p_e,\ e=1,\dots,4\}$. Let $\mathbf{u}\in\mathbf{H}^r(K)$, $0<r<1/2$, $\operatorname{curl}\mathbf{u}\in L^2(K)$, $\operatorname{div}\mathbf{u}=0$. For every $\varepsilon>0$, there exists a constant $C>0$, dependent upon ε but independent of the element and function $\mathbf{u}$, such that*

$$\|\mathbf{u}-\Pi^{\mathrm{curl}}_K\mathbf{u}\|\le C\left(\frac{h}{p}\right)^{(r-\varepsilon)}(\|\mathbf{u}\|_{r,K}+\|\operatorname{curl}\mathbf{u}\|_{0,K}).$$

Here Π^{curl}_K is the projection-based interpolation on K transported from Π^{curl} in (14).

Proof. **Step 1: p-estimate on the master element.** Assume first that $K=\Sigma$ is the master square element. It follows from the integration by parts formula

$$\int_K(\operatorname{curl}\mathbf{u})\phi\,d\mathbf{x}=\int_K\mathbf{u}\cdot\mathbf{curl}\,\phi\,d\mathbf{x}+\int_{\partial K}u_t\phi\,ds$$

that the tangential component u_t lives in $H^{-1/2+r}(\partial K)$ and

$$\|u_t\|_{-1/2+r,\partial K}\le C(\|\mathbf{u}\|_{r,K}+\|\operatorname{curl}\mathbf{u}\|_{0,K}),$$

with C denoting a generic constant depending upon the master element only. We decompose function $\mathbf{u}$ into three contributions

$$\mathbf{u}=\mathbf{u}_1+\mathbf{grad}\,q+\mathbf{u}_3. \tag{28}$$

The terms are constructed as follows.

- $\mathbf{u}_1$ is the lowest degree Whitney interpolant, which means that $\mathbf{u}_1\in\mathbf{N}^{1|\,0}(K)$, $\operatorname{div}\mathbf{u}_1=0$ and the tangential traces of $\mathbf{u}_1$ are the mean values of those of $\mathbf{u}$ on each edge of K.
- Potential q is obtained by integrating tangential component u_t-u_{1t} along the element boundary, starting from any of its vertex nodes. Potential q vanishes at all vertex nodes and
$$\|q\|_{1/2+r,\partial K}\le C\|u_t-u_{1t}\|_{-1/2+r,\partial K}.$$
As the Whitney interpolant depends continuously upon the tangential component u_t itself, and it lives in a finite dimensional space, by the standard finite dimensionality argument we conclude that the norm of potential q is controlled by the norm of $\mathbf{u}$ alone
$$\begin{aligned}\|q\|_{1/2+r,\partial K}&\le C\|u_t\|_{-1/2+r,\partial K}\\&\le C(\|\mathbf{u}\|_{r,K}+\|\operatorname{curl}\mathbf{u}\|_{0,K}).\end{aligned}$$
We extend then potential q to the rest of the element using a harmonic (minimum energy) extension. Consequently,
$$\|q\|_{1+r,K}\le(\|\mathbf{u}\|_{r,K}+\|\operatorname{curl}\mathbf{u}\|_{0,K}).$$

- $\mathbf{u}_3$ is the residual bubble function: $\mathbf{n} \times \mathbf{u}_3 = 0$ on the boundary ∂K, and

$$\operatorname{curl} \mathbf{u}_3 = \operatorname{curl}(\mathbf{u} - \mathbf{u}_1), \quad \operatorname{div} \mathbf{u}_3 = \operatorname{div}(\mathbf{u} - \mathbf{u}_1) = 0.$$

  It follows that $\mathbf{u}_3 \in \mathbf{H}^1(K)$ and

$$\|\mathbf{u}_3\|_{1,K} \leq C \| \operatorname{curl}(\mathbf{u} - \mathbf{u}_1)\|_{0,K} \leq C \| \operatorname{curl} \mathbf{u}\|_{0,K}.$$

We use a similar decomposition for the projection-based interpolant $\Pi_K^{\mathrm{curl}}\mathbf{u}$ of $\mathbf{u}$,

$$\Pi_K^{\mathrm{curl}}\mathbf{u} = \mathbf{u}_1 + \mathbf{grad}\, q_p + \mathbf{u}_{p,3},$$

with the same Whitney interpolant $\mathbf{u}_1$ and $q_p = \Pi_K q$. Thus q_p is only a discrete harmonic function, and $\mathbf{u}_{p,3}$ is only discrete divergence-free. Obviously,

$$\mathbf{u} - \Pi_K^{\mathrm{curl}}\mathbf{u} = \mathbf{grad}(q - q_p) + \mathbf{u}_3 - \mathbf{u}_{p,3}.$$

The first term admits then the estimate (see [16])

$$\begin{aligned} \| \mathbf{grad}(q - q_p)\|_{0,K} &\leq Cp^{-(r-\varepsilon)} \|q\|_{1+r,K} \\ &\leq Cp^{-(r-\varepsilon)} (\|\mathbf{u}\|_{r,K} + \| \operatorname{curl} \mathbf{u}\|_{0,K}). \end{aligned} \tag{29}$$

The estimate of the second term is made possible by Theorem 7: there holds

$$\|\mathbf{u}_3 - \mathbf{u}_{3,p}\|_{0,K} \leq Cp^{1/2} \inf_{\mathbf{F}_{3,p} \in \mathbf{N}_{\mathsf{N}}^p} \|\mathbf{u}_3 - \mathbf{F}_{3,p}\|_{0,K}.$$

The approximation result (27) then gives

$$\begin{aligned} \|\mathbf{u}_3 - \mathbf{u}_{3,p}\|_{0,K} &\leq Cp^{-1/2} \|\mathbf{u}_3\|_{1,K} \\ &\leq Cp^{-1/2} (\|\mathbf{u}\|_{r,K} + \| \operatorname{curl} \mathbf{u}\|_{0,K}). \end{aligned} \tag{30}$$

Combining (29) and (30), we get the final estimate for the master element,

$$\|\mathbf{u} - \Pi_K^{\mathrm{curl}}\mathbf{u}\|_{0,K} \leq Cp^{-(r-\varepsilon)} (\|\mathbf{u}\|_{r,K} + \| \operatorname{curl} \mathbf{u}\|_{0,K}).$$

Step 2: scaling argument. Let K be an arbitrary (unconstrained) square element and let

$$\Sigma = \hat{K} \ni \boldsymbol{\xi} \to \mathbf{x} \in K$$

be the homothetic transformation from the master element Σ onto K. Recalling the transformation for $\mathbf{H}(\mathrm{curl})$-conforming elements,

$$\hat{\mathbf{u}}(\boldsymbol{\xi}) = \mathbf{u}(\mathbf{x}) h \,,$$

where $h = h_K$ is the element size, we follow the standard scaling argument and Step 1 result, to obtain,

$$\begin{aligned} \|\mathbf{u} - \Pi_K^{\mathrm{curl}}\mathbf{u}\|_{0,K} &= \|\hat{\mathbf{u}} - \Pi^{\mathrm{curl}}\hat{\mathbf{u}}\|_{0,\Sigma} \\ &\leq Cp^{-(r-\varepsilon)} (\|\hat{\mathbf{u}}\|_{r,\Sigma} + \| \operatorname{curl} \hat{\mathbf{u}}\|_{0,\Sigma}). \end{aligned}$$

However, the (projection-based) interpolation reproduces polynomials and, by the Bramble-Hilbert argument and standard interpolation arguments, we get

$$\begin{aligned} \|\mathbf{u} - \mathbf{u}_p\|_{0,K} &\leq Cp^{-(r-\varepsilon)} (|\hat{\mathbf{u}}|_{r,\Sigma} + \| \operatorname{curl} \hat{\mathbf{u}}\|_{0,\Sigma}) \\ &\leq C \left(\frac{h}{p}\right)^{(r-\varepsilon)} (|\mathbf{u}|_{r,K} + \| \operatorname{curl} \mathbf{u}\|_{0,K}). \end{aligned}$$

This finishes the proof. □

We have an analogous but slightly different result for element patches.

Lemma 10. *Let P be a patch of two, three or four square elements of same size, forming a rectangle, a L-shaped domain and a square, respectively,* cf *Section* 4.2. *Let p denote the minimum order of all elements and edges constituting the patch. Let h denote the size of the elements forming the patch. Let $\mathbf{u} \in \mathbf{H}^r(P)$, $0 < r < 1/2$, $\operatorname{curl}\mathbf{u} \in L^2(P)$, $\operatorname{div}\mathbf{u} = 0$. There exist constant $C > 0$, independent of the element and function $\mathbf{u}$, and constant r_P, $0 < r_P < r$, such that*

$$\|\mathbf{u} - \Pi_P^{\mathrm{curl}}\mathbf{u}\|_{0,P} \leq C\left(\frac{h}{p}\right)^{r_P}(\|\mathbf{u}\|_{r,P} + \|\operatorname{curl}\mathbf{u}\|_{0,P}).$$

By $\Pi_P^{\mathrm{curl}}\mathbf{u}$ we understand the projection-based interpolation (21) *done on the patch.*

Proof. The reasoning follows the same lines as for the preceding lemma. We revisit the main steps and point out to differences.

- $\mathbf{u}_1$ plays on the patch P a similar (but weaker) role as the lowest degree Whitney interpolant on K: $\mathbf{u}_1 \in \mathbf{N}^{1|\,0}(P)$, $\operatorname{div}\mathbf{u}_1 = 0$ in P and $\mathbf{u}_1$ compensates for the mean value of the tangential trace of $\mathbf{u}$ on the whole boundary ∂P:
$$\int_{\partial P} \mathbf{n} \times (\mathbf{u} - \mathbf{u}_1)\, ds = 0.$$
For $\mathbf{u}_1$ we may take a field of the form $\gamma\mathbf{e}|_P$ where $\mathbf{e}$ is any non-zero element of $\mathbf{N}^{1|\,0}(\hat{P})$ on the convex hull $\hat{P}$ of P, and γ is a suitable constant.
- The potential q is still obtained by first integrating $u_t - u_{1t}$ along ∂P. Now it does not vanish at the corners, but we still have $q \in H^{1/2+r}(\partial P)$, so we can take its harmonic extension in P to find $q \in H^{1+r}(P)$.
- We still have a decomposition like (28) $\mathbf{u} = \mathbf{u}_1 + \mathbf{grad}\, q + \mathbf{u}_3$ with a divergence free patch bubble function $\mathbf{u}_3$. But for the L-shaped patches, $\mathbf{u}_3$ is no longer an $\mathbf{H}^1$-function, however $\mathbf{u}_3$ belongs to $\mathbf{H}^{1/2+r_P}(P)$, with $r_P > 0$ (here r_P is any constant $< \frac{1}{6}$), [12].
- At the discrete level, we have $\Pi_P^{\mathrm{curl}}\mathbf{u} = \mathbf{u}_1 + \mathbf{grad}(\Pi_P q) + \mathbf{u}_{3,p}$. The estimate corresponding to (29), of $\|\mathbf{grad}(q - \Pi_P q)\|_{0,P}$ does not follow directly from element estimates but it can be obtained extending arguments from [16]. Alternatively, the H^1 patch interpolant $\Pi_P q$ can be seen as the Galerkin approximation to the solution of Laplace equation on the patch, with Dirichlet boundary conditions and right approximation of Dirichlet data (in $H^{1/2}$ norm). The corresponding estimates can be found in [30].
- The bound on $\|\mathbf{u}_3 - \mathbf{u}_{3,p}\|_{0,P}$ corresponding to (30) does not follow directly from the L^2- stability result for a single element. Instead, we proceed by comparing the patch interpolant $\mathbf{u}_{3,p} = \Pi_P^{\mathrm{curl}}\mathbf{u}_3$ with the union of interpolants $\Pi_K^{\mathrm{curl}}\mathbf{u}_3$ corresponding to elements K contributing to the patch, denoted by $\mathbf{v}_{3,p}$:
$$\mathbf{v}_{3,p}\big|_K = \Pi_K^{\mathrm{curl}}\mathbf{u}_3, \quad \forall K \subset P.$$
Both operators Π_P^{curl} and $(\Pi_K^{\mathrm{curl}})_{K\subset P}$, acting from $\mathbf{H}_0(\mathrm{curl}, P) \cap \mathbf{H}^\varepsilon(P)$, satisfy the commutativity property for the de Rham diagram. The L^2-projections of $\operatorname{curl}\mathbf{u}$ done

on the whole patch or elementwise, are identical. Consequently,

$$\operatorname{curl} \mathbf{u}_{3,p} = \operatorname{curl} \mathbf{v}_{3,p},$$

and the two functions may differ only by a gradient of potential ϕ that is zero on the patch boundary ∂P and lives in the patch FE space. It follows from the fact that $\mathbf{u}_{3,p}$ is discrete divergence-free that

$$\begin{aligned}\|\mathbf{u}_3 - \mathbf{u}_{3,p}\|_{0,P} &\leq \inf_{\phi} \|\mathbf{u}_3 - \mathbf{u}_{3,p} - \mathbf{grad}\, \phi\|_{0,P} \\ &\leq \|\mathbf{u}_3 - \mathbf{v}_{3,p}\|_{0,P}.\end{aligned}$$

Coming back to the definition of $\mathbf{v}_{3,p}$, we finally obtain

$$\|\mathbf{u}_3 - \mathbf{u}_{3,p}\|_{0,P} \leq \sum_{K \subset P} \|\mathbf{u}_3 - \Pi_K^{\mathrm{curl}} \mathbf{u}_3\|_{0,P}.$$

The estimation can now be done elementwise on each unconstrained element $K \subset P$ utilizing Lemma 9 for $\mathbf{u} := \mathbf{u}_3|_K$, noting that $\operatorname{div} \mathbf{u}_3|_K = 0$.

□

We are ready now to formulate and prove our final result.

Theorem 11. *Starting with a regular mesh on Ω we perform consecutive hp-refinements, enforcing the 1-irregularity and minimum rules, constructing meshes $\mathfrak{M}_{hp}$. We assume that*

$$\max_{K \in \mathfrak{M}_{hp}} \frac{h_K}{p_K} \to 0. \tag{31}$$

Let $\mathbf{u}_{hp} \in \mathbf{X}_{hp}$ be an arbitrary sequence of FE functions on $\mathfrak{M}_{hp}$, such that $\mathbf{u}_{hp} \times \mathbf{n} = 0$ on $\partial\Omega$. We assume that the functions $\mathbf{u}_{hp}$ are discrete divergence free*, i.e.*

$$(\mathbf{u}_{hp}, \mathbf{grad}\, \phi_{hp}) = 0, \quad \forall \phi_{hp} \in \mathbb{Q}_{hp}$$

We also assume that the $\mathbf{u}_{hp}$ are uniformly bounded in the space $\mathbf{H}(\operatorname{curl}, \Omega)$

$$\|\operatorname{curl} \mathbf{u}_{hp}\| \leq 1.$$

Then there exists a subsequence $\mathbf{u}_{hp}$, (denoted with the same symbol) converging strongly in $L^2(\Omega)$ to a limit[1] $\mathbf{u}$

$$\|\mathbf{u}_{hp} - \mathbf{u}\| \to 0.$$

Proof. **Step 1.** Following Kikuchi's reasoning (see [23]), we introduce a sequence of divergence-free functions $\mathbf{u}^{hp}$, satisfying the same essential boundary conditions, such that

$$\operatorname{curl} \mathbf{u}^{hp} = \operatorname{curl} \mathbf{u}_{hp}, \quad (\mathbf{u}^{hp}, \mathbf{grad}\, \phi) = 0 \quad \forall \phi \in H_0^1(\Omega).$$

We have

$$\mathbf{u}_{hp} = \mathbf{u}^{hp} + \mathbf{grad}\, q^{hp}, \tag{32}$$

where q^{hp} is solution to

$$\begin{aligned}&q^{hp} \in H_0^1(\Omega) \\ &(\mathbf{grad}\, q^{hp}, \mathbf{grad}\, \phi) = (\mathbf{u}_{hp}, \mathbf{grad}\, \phi), \quad \forall \phi \in H_0^1(\Omega).\end{aligned}$$

[1]Notice that limit satisfies $\|\operatorname{curl} \mathbf{u}\| \leq 1$, and that $\mathbf{u}$ is (pointwise) divergence-free.

It follows from the regularity results of [12] that

$$\mathbf{u}^{hp} \in \mathbf{H}^r(\Omega),\ r > 0,$$

with a uniform bound on the $\mathbf{H}^r$ norm,

$$\|\mathbf{u}^{hp}\|_{\mathbf{H}^r(\Omega)} \leq C.$$

By a standard compactness argument, there exists a subsequence $\mathbf{u}^{hp}$ converging strongly in $L^2(\Omega)$ to a limit $\mathbf{u}$. We are going to prove that $\mathbf{grad}\, q^{hp} \to 0$, and obtain consequently that $\mathbf{u}_{hp}$ converges to the same limit $\mathbf{u}$.

Step 2. Applying the interpolation operator to both sides of the equation, and using the commutativity of interpolation and the fact that the interpolation preserves FE spaces, we get

$$\mathbf{u}_{hp} = \Pi^{\mathrm{curl}}\mathbf{u}^{hp} + \mathbf{grad}\, \Pi q^{hp}. \tag{33}$$

Subtracting (33) from (32) we get

$$-\mathbf{grad}(q^{hp} - \Pi q^{hp}) = \mathbf{u}^{hp} - \Pi^{\mathrm{curl}}\mathbf{u}^{hp}\ .$$

It follows from (32) that $\mathbf{grad}\, q^{hp}$ is orthogonal to all discrete gradients. Consequently,

$$\|\,\mathbf{grad}\, q^{hp}\| = \inf_{q_{hp}\in Q_{hp}} \|\,\mathbf{grad}(q^{hp} - q_{hp})\| \leq \|\,\mathbf{grad}(q^{hp} - \Pi q^{hp})\| = \|\mathbf{u}^{hp} - \Pi^{\mathrm{curl}}\mathbf{u}^{hp}\|.$$

It is sufficient, therefore, to prove that the interpolation error of functions $\mathbf{u}^{hp}$ converges uniformly to zero.

Step 3. Applying Lemmas 9 and 10, we obtain

$$\begin{aligned}\|\mathbf{u}^{hp} - \Pi^{\mathrm{curl}}\mathbf{u}^{hp}\|^2_{0,\Omega} &= \sum_P \|\mathbf{u}^{hp} - \Pi^{\mathrm{curl}}\mathbf{u}^{hp}\|^2_{0,P} \\ &\leq C\sum_P \left(\frac{h_P}{p_P}\right)^{2r_P} (\|\mathbf{u}^{hp}\|_{r,P} + \|\,\mathrm{curl}\,\mathbf{u}^{hp}\|_{0,P})^2.\end{aligned}$$

Here r is the global regularity constant and $r_P < r$ denote the patch constants discussed in Lemma 10 (we also consider unconstrained elements K as one-element patches and, applying Lemma 9, take r_P as any number between 0 and r in this case) As r_P depends only upon the shape of the patch and the number of different patches is finite, the L^2 interpolation error must converge to zero, if the maximum ratio of patch size and (minimum) order converges to zero,

$$\max_P \frac{h_P}{p_P} \to 0\ .$$

Notice, finally, that the 1-irregularity and max rules imply that the last condition follows from assumption (31). □

Remark 5. Examining our proof, we see that we have proved the following property: There exists a sequence δ_{hp} converging to 0 such that

$$\begin{aligned}&\forall \mathbf{u}_{hp} \in \mathbf{X}_{hp},\ \text{ discrete divergence free,} \\ &\qquad \exists \mathbf{u}^{hp} \in \mathbf{H}_0(\mathrm{curl},\Omega) \text{ with } \mathrm{div}\,\mathbf{u}^{hp} = 0 :\ \|\mathbf{u}^{hp} - \mathbf{u}_{hp}\| \leq C\delta_{hp}(\|\mathbf{u}_{hp}\| + \|\,\mathrm{curl}\,\mathbf{u}_{hp}\|).\end{aligned} \tag{34}$$

Here $C > 0$ does not depend on $\mathbf{u}_{hp}$. Condition (34) implies the discrete compactness property, cf. [3, 4]. It also implies the quasi-optimality of the discrete electric Maxwell problems for any fixed frequency which is not an eigenfrequency of the continuous problem, see [19, 7, 10].

5. Quadrilateral edge elements

In this final section we start a first analysis of the p version of the ABF elements that were introduced to help with some of the difficulties related to general quadrilateral meshes. A recent result (see [2]) shows that two dimensional Raviart–Thomas elements do not achieve optimal approximation properties in the $\mathbf{H}(\mathrm{div})$ norm on general quadrilateral meshes. Since in this case the divergence operator is isomorphic to the curl one and since, under this canonical isomorphism, the Raviart–Thomas spaces correspond to the Nedelec first family of edge elements, the result of [2] shows that Nedelec elements are not optimal for computing Maxwell's eigenvalues on general quadrilateral meshes. For more information on quadrilateral edge elements for the h version, we refer to [2, 20, 8].

One of the possible cures is to use an augmented version of edge element spaces introduced in [2]. In this section, we extend the results of Section 3, thus showing that this new family of finite elements provides convergent and spurious mode free approximation to Maxwell's eigenvalues.

The following investigations are mainly theoretical with rather technical proofs. We hope that the results presented in this section can be of some help for further research on hp convergence using general quadrilateral meshes.

Let $\mathbf{A}^p(\Sigma)$ denote the augmented space $\mathbb{Q}^{p-1,p+1}(\Sigma) \times \mathbb{Q}^{p+1,p-1}(\Sigma)$ introduced in [2]. Its subspace $\mathbf{A}^p_{\mathsf{N}}(\Sigma)$ of fields satisfying the electric boundary condition is given by

$$\mathbf{A}^p_{\mathsf{N}}(\Sigma) = \big[\mathbb{P}^{p-1}(I) \otimes \mathbb{P}^{p+1}_0(I)\big] \times \big[\mathbb{P}^{p+1}_0(I) \otimes \mathbb{P}^{p-1}(I)\big]. \tag{35}$$

The Maxwell spectrum in $\mathbf{A}^p_{\mathsf{N}}(\Sigma)$ is formed by the eigenpairs $(\lambda, \mathbf{u})$:

$$\mathbf{u} \in \mathbf{A}^p_{\mathsf{N}}(\Sigma) \setminus \{0\} : \quad \int_\Sigma \operatorname{curl} \mathbf{u} \, \operatorname{curl} \mathbf{v} \, d\mathbf{x} = \lambda \int_\Sigma \mathbf{u} \cdot \mathbf{v} \, d\mathbf{x}, \quad \forall \mathbf{v} \in \mathbf{A}^p_{\mathsf{N}}(\Sigma). \tag{36}$$

We study the spectrum in $\mathbf{A}^p_{\mathsf{N}}(\Sigma)$ in a heuristic and constructive way following the notation introduced in Section 3 (see, in particular, Theorem 1).

We first note the obvious presence of the parts **(a)** and **(b)** of the spectrum:

- **(a)** The kernel is $\mathbf{grad}(\mathbb{P}^p_0 \otimes \mathbb{P}^p_0)$ with dimension $(p-1)^2$.
- **(b)** Each Dirichlet discrete eigenvalue $\lambda_j^{[p+1]}$, $j = 1, \dots, p$, belongs to the spectrum and is associated with the two eigenvectors $\big(0, -\beta_j^{[p+1]}(x)\big)$ and $\big(\beta_j^{[p+1]}(y), 0\big)$. The sum of the dimensions of the corresponding eigenspaces is $2p$.

Now, we are going to identify the eigenmodes corresponding to part **(c)**: We construct successively the simple eigenvalues and the remaining double eigenvalues of problem (36), linking all of them with 1D eigenvalues.

Let T be the operator

$$T\big(v(x,y), w(x,y)\big) = \big(w(y,x), v(y,x)\big)$$

It is clear that T is a *symmetry* and that it *commutes* with the operator $\mathbf{curl}\,\mathrm{curl}$. Moreover, it acts from $\mathbf{A}^p_{\mathsf{N}}(\Sigma)$ into itself, (see (35)). Therefore, the operator $\mathbf{curl}\,\mathrm{curl}$ possesses a basis of eigenvectors $\mathbf{u}$ which are also eigenvectors for T, i.e., satisfy

$$T\mathbf{u}=\mathbf{u} \quad \text{or} \quad T\mathbf{u}=-\mathbf{u}, \quad \text{i.e.,} \quad \mathbf{u}=\big(v(x,y),\varepsilon v(y,x)\big), \quad \text{with} \quad \varepsilon=\pm 1.$$

5.1. **Simple eigenvalues.**

5.1.1. *Ansatz.* Let us look for eigenvectors of the form above with $v(x,y)=a(x)b(y)$, $a\in\mathbb{P}^{p-1}(I)$ and $b\in\mathbb{P}^{p+1}_0(I)$. The equation $\int_\Sigma(\mathbf{curl}\,\mathrm{curl}\,\mathbf{u}-\lambda\mathbf{u})\breve{\mathbf{u}}=0$ for all $\breve{\mathbf{u}}\in\mathbf{A}^p_{\mathsf{N}}(\Sigma)$ becomes

$$\int_\Sigma \Big(-a(x)b''(y)+\varepsilon b'(x)a'(y)-\lambda a(x)b(y)\Big)\breve{a}(x)\breve{b}(y)\,dxdy=0, \qquad \forall \breve{a}\in\mathbb{P}^{p-1}(I), \quad \forall\breve{b}\in\mathbb{P}^{p+1}_0(I). \tag{37}$$

We write $b'(x)=a(x)+(b'(x)-a(x))$, and we note that (37) is satisfied in particular if

$$\begin{aligned}&\int_I \Big(-b''(y)+\varepsilon a'(y)-\lambda b(y)\Big)\breve{b}(y)\,dy=0, \quad \forall\breve{b}\in\mathbb{P}^{p+1}_0(I)\\ &\int_I \Big(b'(x)-a(x)\Big)\breve{a}(x)\,dx=0, \quad \forall\breve{a}\in\mathbb{P}^{p-1}(I).\end{aligned} \tag{38}$$

Problem (38) is an eigenvalue problem for a mixed problem on the interval I. We will interpret it as a spectral problem for a self-adjoint operator. Let us denote by P the orthogonal projection in $L^2(I)$ on the space $\mathbb{P}^{p-1}(I)$. Let D denote the operator $b\mapsto b'$. The second line of (38) can be interpreted as $a=\mathrm{P}\mathrm{D}b$. Using that equality in the first line, and integrating by parts we find

$$\int_I \mathrm{D}b\,\mathrm{D}\breve{b}-\varepsilon\mathrm{P}\mathrm{D}b\,\mathrm{D}\breve{b}=\lambda\int_I b\,\breve{b}, \quad \forall\breve{b}\in\mathbb{P}^{p+1}_0(I).$$

In fact, as P is a projection, we equivalently have

$$\int_I \mathrm{D}b\,\mathrm{D}\breve{b}-\varepsilon\mathrm{P}\mathrm{D}b\,\mathrm{P}\mathrm{D}\breve{b}=\lambda\int_I b\,\breve{b}, \quad \forall\breve{b}\in\mathbb{P}^{p+1}_0(I). \tag{39}$$

Let us introduce the two operators

$$\begin{aligned}&A:\mathbb{P}^{p+1}_0(I)\longrightarrow\mathbb{P}^{p+1}_0(I)', \quad b\longmapsto\Big(\breve{b}\to\int_I \mathrm{D}b\,\mathrm{D}\breve{b}\Big)\\ &B:\mathbb{P}^{p+1}_0(I)\longrightarrow\mathbb{P}^{p+1}_0(I)', \quad b\longmapsto\Big(\breve{b}\to\int_I \mathrm{P}\mathrm{D}b\,\mathrm{P}\mathrm{D}\breve{b}\Big).\end{aligned} \tag{40}$$

Note that A is the discrete Dirichlet operator.

Then, equation (39) can alternatively be written as

$$Ab-\varepsilon Bb=\lambda\,b. \tag{41}$$

5.1.2. *Kernel of B.* At this point we need results on $\ker B$ and on how A behaves on $\ker B$.

Lemma 12. (i) *The kernel of B is one dimensional and generated by the primitive $K_p \in \mathbb{P}_0^{p+1}(I)$ of the Legendre polynomial L_p.*
(ii) *We have the formula*

$$K_p = \frac{1}{2p+1}\,(L_{p+1} - L_{p-1}). \tag{42}$$

(iii) *The polynomial K_p is not an eigenvector of A.*
(iv) *We denote by λ_0 the Rayleigh quotient of A associated with K_p:*

$$\lambda_0 := \Big(\int_I |L_p|^2\Big)\Big(\int_I |K_p|^2\Big)^{-1}. \tag{43}$$

There holds

$$\lambda_0 = \frac{(2p+3)(2p-1)}{2}\,. \tag{44}$$

Proof. (i) The kernel of B is the set of $b \in \mathbb{P}_0^{p+1}(I)$ such that PDb is zero. This means that b' is orthogonal to $\mathbb{P}^{p-1}(I)$. Therefore, and since b' is of degree p, it is proportional to L_p. Finally b is the unique primitive of L_p which is zero at 1 (then, since L_p is orthogonal to constants, such a primitive is zero at -1 as well).
(ii) Let us denote by $J_N^{\alpha,\alpha}$ the Jacobi polynomial of degree N associated with the weight $(1-x^2)^\alpha$. There holds (Rodrigues' formula)

$$J_N^{\alpha,\alpha} = a_N^{-1}(1-x^2)^{-\alpha}\frac{d^N}{dx^N}\Big((1-x^2)^{N+\alpha}\Big) \quad \text{with} \quad a_N = (-1)^N 2^N N!.$$

Applying this formula for $\alpha = 0$ and 1, we obtain

$$K_p = a_p^{-1}\frac{d^{p-1}}{dx^{p-1}}\Big((1-x^2)^p\Big) = \frac{a_{p-1}}{a_p}\,(1-x^2)J_{p-1}^{1,1}.$$

Then formula (42) can be deduced from classical recurrence relations [1, (22.5.15 & 16)].
(iii) With $b = K_p$ and for all $\breve{b} \in \mathbb{P}_0^p(I)$, we have $\int_I \mathrm{D}b\,\mathrm{D}\breve{b} = \int_I L_p\,\breve{b}' = 0$ since the degree of $\breve{b}'$ is $p-1$. If K_p was an eigenvector of A, then $\int_I b\,\breve{b} = 0$ for all $\breve{b} \in \mathbb{P}_0^p(I)$, which means that $b/(1-x^2)$ is proportional to the Jacobi polynomial $J_{p-1}^{2,2}$. In other words, K_p would be proportional to $(1-x^2)J_{p-1}^{2,2}$. But we have just seen that K_p is proportional to $(1-x^2)J_{p-1}^{1,1}$. Since $J_N^{1,1}$ is not proportional to $J_N^{2,2}$ for any $N \geq 2$, we have obtained the contradiction.
(iv) There holds $\|L_p\|^2_{L^2(I)} = (p+\frac{1}{2})^{-1}$. Combined with (42), we find (44). □

5.1.3. *Construction of simple eigenpairs.*

(i) Case when $\varepsilon = -1$: Then the operator $A+B$ in (41) is > 0 on $\mathbb{P}_0^{p+1}(I)$. It has p non-zero eigenvalues μ_j^+, corresponding to eigenvectors b_j^+. We note that the only polynomial b, for which $a = \mathrm{PD}b$ is zero, is K_p and equation (41) would become $AK_p = \lambda K_p$, which does not hold by Lemma 12. Therefore, all the $a_j^+ := \mathrm{PD}b_j^+$ are non-zero, and we have found the eigenpairs

$$\lambda = \mu_j^+, \quad \mathbf{u}_j^+ = \big(a_j^+(x)b_j^+(y), -b_j^+(x)a_j^+(y)\big).$$

(ii) Case when $\varepsilon = 1$: for all $b \in \mathbb{P}_0^p$, PDb = Db. Therefore $\lambda = 0$ is eigenvalue of the operator $A-B$ with multiplicity $\geq p-1$. Since, nevertheless, this operator is not $\equiv 0$ and

acts between spaces of dimension p, it has a unique non-zero eigenvalue $\mu_p^- > 0$ and we have found the eigenpair

$$\lambda = \mu_p^-, \quad \mathbf{u}_p^- = \big(a_p^-(x)b_p^-(y), b_p^-(x)a_p^-(y)\big).$$

Since the Rayleigh quotient of K_p is the same for $A - B$ and for B, we obtain the inequality (see (43))

$$\lambda_0 \leq \mu_p^-,$$

which provides the lower bound $O(p^2)$ for this μ_p^- (see (44)).

Remark 6. The polynomial $(1-x^2)J_{p-1}^{2,2}$ is an eigenvector of $A - B$ for the eigenvalue μ_p^-.

In fact, we know more about the eigenvalues μ_j^+ by arguments of *parity*: indeed, the projection operator P does not modify the parity.

Since the subspace of $\mathbb{P}_0^{p+1}$ of polynomials which have the parity of p is contained in $\mathbb{P}^p$, B coincides with A on this subspace. Hence, all eigenvalues μ_j^+ corresponding to this parity are eigenvalues of the operator $2A$. Therefore, there exist ranks $n(j)$ such that

$$\mu_{n(1)}^+ = 2\lambda_1^{[p+1]}, \quad \mu_{n(3)}^+ = 2\lambda_3^{[p+1]}, \ldots, \quad \mu_{n(p-1)}^+ = 2\lambda_{p-1}^{[p+1]} \quad \text{if } p \text{ is even}$$
$$\mu_{n(2)}^+ = 2\lambda_2^{[p+1]}, \quad \mu_{n(4)}^+ = 2\lambda_{n(4)}^{[p+1]}, \ldots, \quad \mu_{n(p-1)}^+ = 2\lambda_{p-1}^{[p+1]} \quad \text{if } p \text{ is odd.}$$

In Tables 1 and 2 we report the computed values of $4\lambda_j/\pi^2$ (thus, eigenvalues corresponding to the interval $(0,\pi)$) for $p = 1, \ldots, 8$, and, in Table 3, the values of $4\lambda_0/\pi^2$. Note that $\lambda_0 \neq \lambda_j$ for $j = 1, \ldots, p$ in this range of values.

TABLE 1. Dirichlet discrete eigenvalues (operator A).

p	$4\lambda_1/\pi^2$	$4\lambda_2/\pi^2$	$4\lambda_3/\pi^2$	$4\lambda_4/\pi^2$
1	1.013211836423			
2	1.013211836423	4.255489712978		
3	1.000014713885	4.255489712978	10.34795785406	
4	1.000014713885	4.002344086420	10.34795785406	20.31473998774
5	1.000000003434	4.002344086420	9.03517709781	20.31473998774
6	1.000000003434	4.000005652740	9.03517709781	16.21057025598
7	1.000000000000	4.000005652740	9.00030685779	16.21057025598
8	1.000000000000	4.000000004821	9.00030685779	16.00438657110

TABLE 2. Dirichlet discrete eigenvalues (operator A), continued.

p	$4\lambda_5/\pi^2$	$4\lambda_6/\pi^2$	$4\lambda_7/\pi^2$	$4\lambda_8/\pi^2$
5	35.55935553780			
6	35.55935553780	57.80673549588		
7	25.77791686519	57.80673549588	89.04947452438	
8	25.77791686519	38.14483931939	89.04947452438	131.52402988315

TABLE 3. Rayleigh quotient of A on the kernel of B.

p	$4\lambda_0/\pi^2$
1	1.013211836423
2	4.255489712978
3	9.118906527810
4	15.60346227248
5	23.70915602086
6	33.43599465559
7	44.78396152169
8	57.75307717678

5.2. **Double eigenvalues.**

5.2.1. *Ansatz.* To formulate the Ansatz, let us consider the pairs of eigenvectors (8) associated with (j,k) and (k,j) for $j \neq k$. Considering their sum and difference, we see that we have a pair of eigenvectors of the form

$$\begin{aligned} &\big(a(x)b(y) + c(x)d(y), -b(x)a(y) - d(x)c(y)\big) \\ &\big(a(x)b(y) - c(x)d(y),\ \ b(x)a(y) - d(x)c(y)\big) \end{aligned} \tag{45}$$

which are also eigenvectors of the symmetry T associated with the eigenvalues 1 and -1, respectively. Thus, we will consider (45) as Ansatz, together with the assumption that they are associated with the *same* eigenvalue λ. We obtain the system

$$\begin{aligned} &\int_\Sigma \Big(- a(x)b''(y) - c(x)d''(y) - b'(x)a'(y) - d'(x)c'(y) \\ &\qquad - \lambda a(x)b(y) - \lambda c(x)d(y)\Big)\breve{a}(x)\breve{b}(y)\,dxdy = 0, \quad \forall \breve{a} \in \mathbb{P}^{p-1}(I), \quad \forall \breve{b} \in \mathbb{P}_0^{p+1}(I) \\ &\int_\Sigma \Big(- a(x)b''(y) + c(x)d''(y) + b'(x)a'(y) - d'(x)c'(y) \\ &\qquad - \lambda a(x)b(y) + \lambda c(x)d(y)\Big)\breve{c}(x)\breve{d}(y)\,dxdy = 0, \quad \forall \breve{c} \in \mathbb{P}^{p-1}(I), \quad \forall \breve{d} \in \mathbb{P}_0^{p+1}(I). \end{aligned}$$

Using the operators A and B we can write the above system as

$$\begin{aligned} &a(x)\,Ab(y) + c(x)\,Ad(y) - \mathrm{PD}b(x)\,a'(y) - \mathrm{PD}d(x)\,c'(y) = \lambda a(x)b(y) + \lambda c(x)d(y) \\ &a(x)\,Ab(y) - c(x)\,Ad(y) + \mathrm{PD}b(x)\,a'(y) - \mathrm{PD}d(x)\,c'(y) = \lambda a(x)b(y) - \lambda c(x)d(y). \end{aligned} \tag{46}$$

Now, we write

$$\mathrm{PD}b(x) = \rho c(x) + (\mathrm{PD}b(x) - \rho c(x)) \quad \text{and} \quad \mathrm{PD}d(x) = \varepsilon\rho^{-1}a(x) + (\mathrm{PD}d(x) - \varepsilon\rho^{-1}a(x))$$

with a coefficient $\rho \geq 1$ and $\varepsilon = \pm 1$, and we note that (37) is satisfied in particular if

$$\begin{aligned} Ab'' - \varepsilon\rho^{-1}c' &= \lambda\, b, \\ Ad'' - \rho a' &= \lambda\, d, \\ \mathrm{PD}d - \varepsilon\rho^{-1}a &= 0, \\ \mathrm{PD}b - \rho c &= 0. \end{aligned} \tag{47}$$

The last two lines of (47) can be written as

$$a = \varepsilon\rho \mathrm{PD} d \quad \text{and} \quad c = \rho^{-1}\mathrm{PD} b.$$

Then the first two lines of (47) become

$$Ab + \varepsilon\rho^{-2} Bb = \lambda\, b \quad \text{and} \quad Ad + \varepsilon\rho^{2} Bd = \lambda\, d,$$

which means that we are looking for the values of ρ so that the operators $A + \varepsilon\rho^{-2}B$ and $A + \varepsilon\rho^{2}B$ have a common eigenvalue. For $\sigma \geq 0$, let us denote by

$$\begin{aligned} &\mu_1^+[\sigma] \leq \ldots \leq \mu_p^+[\sigma] \qquad \text{the eigenvalues of} \quad A + \sigma B, \\ &\mu_1^-[\sigma] \leq \ldots \leq \mu_p^-[\sigma] \qquad \text{the eigenvalues of} \quad A - \sigma B. \end{aligned} \tag{48}$$

The eigenvalues of A are denoted by $\lambda_1 < \ldots < \lambda_p$ (we drop the exponent $[p+1]$) and the eigenvalues of B are denoted by $\nu_1 < \nu_2 \leq \ldots \leq \nu_p$, with $\nu_1 = 0$.

Lemma 13. *(i) For all $\sigma > 0$, the functions $\mathbb{R}^+ \ni \sigma \mapsto \mu_j^+[\sigma]$ and $\mathbb{R}^+ \ni \sigma \mapsto \mu_j^-[\sigma^{-1}]$ are increasing and we have the inequalities*

$$\begin{aligned} &\max\{\lambda_j, \sigma\nu_j\} < \mu_j^+[\sigma] \leq (1+\sigma)\lambda_j, \qquad &&\sigma > 0 \\ &0 \leq \mu_j^-[\sigma^{-1}] \leq \lambda_j, &&\sigma \geq 1. \end{aligned} \tag{49}$$

(ii) The parity argument yields that there exist ranks $n(j)$ (depending on σ)

$$\mu^{\pm}_{n(p-1-2k)}[\sigma] = (1 \pm \sigma)\lambda_{p-1-2k}, \quad k = 0, 1, \ldots, \left[\tfrac{p-1}{2}\right]. \tag{50}$$

(iii) If λ_0 is the Rayleigh quotient of A associated with the kernel of B, (see (43)), then there holds

$$\lim_{\sigma\to+\infty} \mu_1^+[\sigma] = \lambda_0 \quad \textit{and} \quad \lim_{\sigma\to+\infty} \mu_p^-[\sigma] = \lambda_0. \tag{51}$$

Proof. (i) and (ii) are more or less obvious. (iii) The operators $B \pm \sigma^{-1}A$ have the same eigenvectors as $A \pm \sigma B$. We can study the spectrum of $B \pm \sigma^{-1}A$ by the method of asymptotic expansion. Let us set $h := \pm\sigma^{-1}$. We are looking for the eigenvalue $\nu(h)$ of $B + hA$ which tends to zero as $h \to 0$. We set $\nu(h) = h\nu_0 + O(h^2)$ and make the Ansatz $b(h) = b_0 + hb_1 + O(h^2)$ for the eigenvector. The equation $(B + hA)b(h) = \nu(h)b(h)$ provides the relations

$$Bb_0 = 0 \quad \text{and} \quad Bb_1 + Ab_0 = \nu_0 b_0.$$

Since B is self-adjoint, its range is orthogonal to its kernel, therefore $\langle Bb_1, b_0\rangle = 0$, which yields the relation

$$\langle Ab_0, b_0\rangle = \nu_0 \langle b_0, b_0\rangle,$$

which, together with (43), implies that $\nu_0 = \lambda_0$. Thus, the eigenvalue of $B \pm \sigma^{-1}A$ which tends to zero as $\sigma \to +\infty$, has the form $\pm\sigma^{-1}\lambda_0 + O(\sigma^{-2})$. The corresponding eigenvalue of $A \pm \sigma B$ is $\lambda_0 + O(\sigma^{-1})$. Since B is non-negative, this eigenvalue is the first one of $A + \sigma B$ and the last one of $A - \sigma B$. □

5.2.2. *Construction of double eigenpairs.*

(i) Case when $\varepsilon = 1$. From (49), we know that $\mu_2^+[\sigma]$ tends to $+\infty$ as $\sigma \to \infty$. The functions $\sigma \mapsto \mu_j^+[\sigma^{-1}]$ are decreasing. In the interval $(1, +\infty)$, the function $\sigma \mapsto \mu_2^+[\sigma]$ crosses the functions $\sigma \mapsto \mu_j^+[\sigma^{-1}]$ for all $j = 3, \dots, p$ because $\mu_j^+[1] > \mu_2^+[1]$. Let $\sigma_{2,j}^+$ be the value of σ such that $\mu_2^+[\sigma] = \mu_j^+[\sigma^{-1}]$.

In the same way, we find that $\sigma \mapsto \mu_3^+[\sigma]$ crosses the functions $\sigma \mapsto \mu_j^+[\sigma^{-1}]$ for all $j = 4, \dots, p$ at points $\sigma_{3,j}^+$. Continuing in that way, we find

$$p - 2 + p - 3 + \ldots + 1 = (p-2)(p-1)/2$$

pairs of eigenvectors.

Concerning $\mu_1^+[\sigma]$, it goes from $\mu_1^+[1]$ to its limit λ_0 as σ goes from 1 to $+\infty$. We know that $\mu_j^+[\sigma^{-1}] \searrow \lambda_j$ (the j-th eigenvalue of A) as $\sigma \to +\infty$ and starting from $\mu_j^+[1]$ as $\sigma = 1$. Therefore we have a cross point $\sigma_{1,j}^+$ for each $j \geq 2$ such that $\lambda_j < \lambda_0$.

(ii) Case when $\varepsilon = -1$. $\mu_j^-[\sigma^{-1}] \nearrow \lambda_j$ as $\sigma \to +\infty$, starting from $\mu_j^-[1]$ as $\sigma = 1$. In other words, $\mu_j^-[\sigma^{-1}]$ goes from 0 to λ_j for $j = 1, \dots, p-1$, and from μ_p^- to λ_p for $j = p$. When $\sigma > 1$, $\mu_j^-[\sigma] < \mu_j^-[1] = 0$, $j = 1, \dots, p-1$ and $\mu_p^-[\sigma] \searrow \lambda_0$, *cf* (51), starting from μ_p^-. Therefore we have a cross point $\sigma_{p,j}^-$ for each $j \leq p-1$ such that $\lambda_j > \lambda_0$.

(iii) The unlikely case when there exists $j \in \{1, \dots, p\}$ such that $\lambda_0 = \lambda_j$ (we have no proof that it is impossible). In that situation, we solve (46) explicitly. We take the eigenvector β_j for d, the kernel element K_p for b, we set $a = \mathrm{PD}\beta_j$ and $c = \mathrm{PD}b_1$, where b_1 solves

$$Bb_1 = \lambda_0 b - Ab.$$

In fact b_1 was introduced in the proof of Lemma 13 above. Setting $\lambda = \lambda_0 = \lambda_j$, we therefore have the following relations:

$$a = \mathrm{PD}d, \quad \mathrm{PD}b = 0, \quad c' = Ab - \lambda b, \quad Ad = \lambda d.$$

Relations (46) are now straightforward.

5.3. **Conclusion and proof of convergence.** We have now collected all eigenvectors. We use the notation introduced in (40), (43), and (48). We recall that $(\lambda_j^{[p+1]}, \beta_j^{[p+1]})$ are the eigenpairs of the discrete Dirichlet operator A on $\mathbb{P}_0^{p+1}$.

Theorem 14. *The whole Maxwell spectrum* (36) *in* $\mathbf{A}_{\mathsf{N}}^p(\Sigma)$ *is characterized by the following three families of eigenmodes.*

- **(a)** *The kernel:* $\lambda = 0$ *and* $\mathbf{u} \in \mathbf{grad}(\mathbb{P}_0^p \otimes \mathbb{P}_0^p)$.
- **(b)** *The Dirichlet discrete eigenvalues* $\lambda_j^{[p+1]}$ *associated with the two eigenvectors*

$$\big(0, -\beta_j^{[p+1]}(x)\big) \quad \textit{and} \quad \big(\beta_j^{[p+1]}(y), 0\big).$$

- **(c)** *Simple and double eigenvalues according to*

Simple (s^+) *The eigenvalues* $\mu_j^+[1]$ *of* $A + B$, $j = 1, \dots, p$.

(s^-) *The non-zero eigenvalue* $\mu_p^-[1]$ *of* $A - B$; *there holds* $\mu_p^-[1] > \lambda_0$.

Double (d^+) *The eigenvalues* $\mu_j^+[\sigma_{j,k}^+] = \mu_k^+[1/\sigma_{j,k}^+]$

(i) *for* $j = 1$ *and* $k \geq 2$ *such that* $\lambda_k^{[p+1]} < \lambda_0$,

(ii) *for* $2 \leq j < k \leq p$,

(d^-) *The eigenvalues* $\mu_p^-[\sigma_{p,k}^-] = \mu_k^-[1/\sigma_{p,k}^-]$ *for* $k \leq p-1$ *such that* $\lambda_k^{[p+1]} > \lambda_0$. *These eigenvalues are* $> \lambda_0$.

(d^0) *The eigenvalue* λ_0 *if there exists* j, $\lambda_j = \lambda_0$.

Proof. We easily check that the number of eigenvalues that we have constructed is

$$(p-1)^2 + 2p + p + 1 + (p-2)(p-1) + 2(p-2) = 2p^2 = \dim \mathbf{A}_{\mathsf{N}}^p(\Sigma).$$

□

Remark 7. For those pairs $\mu_j^+[\sigma_{j,k}^+] = \mu_k^+[1/\sigma_{j,k}^+]$ which corresponds to eigenvectors *which have the parity of* p, there holds (see (50))

$$\mu_j^+[\sigma_{j,k}^+] = (1+\sigma_{j,k}^+)\lambda_{j'}^{[p+1]} \quad \text{and} \quad \mu_k^+[1/\sigma_{j,k}^+] = (1+1/\sigma_{j,k}^+)\lambda_{k'}^{[p+1]}.$$

The equality $\mu_j^+[\sigma_{j,k}^+] = \mu_k^+[1/\sigma_{j,k}^+]$ yields that $\sigma = \lambda_{k'}^{[p+1]}/\lambda_{j'}^{[p+1]}$, whence

$$\mu_j^+[\sigma_{j,k}^+] = \mu_k^+[1/\sigma_{j,k}^+] = \lambda_{j'}^{[p+1]} + \lambda_{k'}^{[p+1]}.$$

This formula is similar to family **(c)** for the edge element $\mathbf{N}_{\mathsf{N}}^p(\Sigma)$.

It is clear that, in order to prove the convergence of eigenvalues/eigenvectors in **(a)**, **(b)**, and **(c)** towards those of Maxwell eigenproblem, we need to show that, in a sense to be made more precise, the eigenvalues/eigenvectors in **(c)** are a good approximation of the corresponding eigenvalues/eigenvectors in **(c)** of Section 2.2. Indeed, **(a)** represents the kernel of the operator and **(b)** contains eigenvalues/eigenvectors which are known to provide a good approximation to the corresponding ones of the continuous problem.

We will examine in more detail the convergence of those eigenvalues in **(c)** which are smaller than λ_0. This is because λ_0, as shown in the previous section, increases fast with p (namely, it is of order p^2) and the eigenvalues larger that it can be disregarded from this discussion, since we are interested in the approximation of a fixed (possibly large) number of eigenvalues as p tends to infinity. Hence, we consider neither the simple eigenvalue $\mu_p^-[1]$ in sub-family (s^-), nor the double eigenvalues $\mu_p^-[\sigma_{p,k}^-] = \mu_k^-[1/\sigma_{p,k}^-]$ in sub-family (d^-), since all are larger than λ_0. The next lemma states that the eigenvalues/eigenvectors of the operator $A + \sigma B$ approximate those of $(1+\sigma)A$, for any $\sigma \geq 0$.

Lemma 15. *Given* $N \in \mathbb{N}$ *and* $\sigma \geq 0$, *as* p *goes to infinity, the difference between the first* N *eigenvalues of the operator* $A + \sigma B$ *and the first* N *eigenvalues of the operator* $(1+\sigma)A$ *tends to zero.*

Proof. Let $\sigma = \rho^2, \rho \in \mathbb{R}$. Given $f \in L^2(I)$, let us introduce the following variational problem: find $u \in H_0^1(I)$ and $s \in L^2(I)$ such that

$$\begin{aligned} &(u', v') + \rho(v', s) = (f, v) && \forall v \in H_0^1(I) \\ &\rho(u', t) - (s, t) = 0 && \forall t \in L^2(I), \end{aligned} \tag{52}$$

where $(\cdot,\cdot)$ denotes the $L^2(I)$ scalar product. It is not difficult to see that equation (52) is a (unusual) weak form of the problem

$$-(1+\sigma)u'' = f \quad \text{in } I, \qquad u(\pm 1) = 0.$$

If we call T the resolvent operator associated with the 1D Dirichlet problem, then we can write

$$\begin{aligned} &(\frac{1}{1+\sigma}\,(Tf)', v') + \rho(v', s) = (f, v) && \forall v \in H^1_0(I) \\ &(\frac{\rho}{1+\sigma}\,(Tf)', t) - (s, t) = 0 && \forall t \in L^2(I). \end{aligned}$$

Let us now introduce a discretization of problem (52) as follows: find $b \in \mathbb{P}^{p+1}_0(I)$ and $a \in \mathbb{P}^{p-1}(I)$ such that

$$\begin{aligned} &(b', \breve{b}') + \rho(\breve{b}', a) = (f, \breve{b}) && \forall \breve{b} \in \mathbb{P}^{p+1}_0(I) \\ &\rho(b', \breve{a}) - (a, \breve{a}) = 0 && \forall \breve{a} \in \mathbb{P}^{p-1}(I), \end{aligned} \tag{53}$$

where the analogies with equations (38) and (47) are evident. Problem (53) is uniquely solvable, a stability estimate is easily obtained by taking $\breve{b} = b$ in the first equation and subtracting the second one with $\breve{a} = a$, and the following error estimate holds true

$$\|u - b\|_{1,I} + \|s - a\|_{0,I} \le C \inf_{\breve{b} \in \mathbb{P}^{p+1}_0(I),\ \breve{a} \in \mathbb{P}^{p-1}(I)} \left(\|u - \breve{b}\|_{1,I} + \|s - \breve{a}\|_{0,I} \right). \tag{54}$$

Define the discrete resolvent operator $T_p : L^2(I) \to L^2(I)$ by the solution of (53):

$$T_p f = (1+\sigma) b\,.$$

Then the error estimate (54) and standard regularity results imply the convergence

$$\|T - T_p\|_{\mathcal{L}(L^2(I))} \to 0 \tag{55}$$

as $p \to \infty$.

We now consider the eigenvalue problem associated with (53), namely: Find $\lambda \in \mathbb{R}$, $b \in \mathbb{P}^{p+1}_0(I)$ with $b \not\equiv 0$, and $a \in \mathbb{P}^{p-1}(I)$ such that

$$\begin{aligned} &(b', \breve{b}') + \rho(\breve{b}', a) = \lambda(b, \breve{b}) && \forall \breve{b} \in \mathbb{P}^{p+1}_0(I) \\ &\rho(b', \breve{a}) - (a, \breve{a}) = 0 && \forall \breve{a} \in \mathbb{P}^{p-1}(I). \end{aligned} \tag{56}$$

An integration by parts in equation (38) shows that the eigenvalues/eigenspaces of (56) coincide with those of (38) with $\varepsilon = -1$ and B replaced by σB. Moreover, they are equivalent to the eigenvalues/eigenspaces of the operator $A + \sigma B$. A consequence of the uniform convergence (55) is that the eigenvalues/eigenspaces of (56) converge to those of the operator $(1+\sigma)T^{-1}$.

Since we know that the eigenvalues/eigenspaces of the operator A converge to those of T^{-1}, we can conclude that the eigenvalues/eigenspaces of $A+\sigma B$ and those of $(1+\sigma)A$ tend to the same limits. □

The previous result shows, in particular, that simple eigenvalues $\mu^+_j[1]$ in **(c)** converge to true Maxwell eigenvalues.

Another immediate consequence is that those eigenvalues $\mu_j^+[\sigma_{j,k}^+] = \mu_k^+[1/\sigma_{j,k}^+]$ which correspond to eigenvectors having the same parity of p converge to true Maxwell eigenvalues; indeed we had shown that their values are equal to $\lambda_{j'}^{[p+1]} + \lambda_{k'}^{[p+1]}$.

In order to prove the expected convergence of all eigenvalues smaller than λ_0, we need to show that also the other eigenvalues of the family $\mu_j^+[\sigma_{j,k}^+] = \mu_k^+[1/\sigma_{j,k}^+]$ provide correct approximation of true Maxwell eigenvalues. In order to do so, let us proceed as follows. From the identity $\mu_j^+[\sigma_{j,k}^+] = \mu_k^+[1/\sigma_{j,k}^+]$, the definition of $\mu_j^+[\sigma]$, and the previous lemma, we get

$$(1 + \sigma(1 + \delta_j))\lambda_j = (1 + \sigma(1 + \delta_k))\lambda_k$$

where δ_j and δ_k are small perturbations tending to zero as p goes to infinity. Solving this equation for σ gives, after easy computations,

$$\sigma = \frac{\lambda_k}{\lambda_j}(1 + \delta)$$

with δ tending to zero as p goes to infinity. Putting things together, we obtain that the values $\mu_j^+[\sigma_{j,k}^+] = \mu_k^+[1/\sigma_{j,k}^+]$ tend to $\lambda_{j'}^{[p+1]} + \lambda_{k'}^{[p+1]}$ for suitable indices j' and k'. We have all the ingredients to state the following theorem.

Theorem 16. *Given $N \in \mathbb{N}$, the first N positive eigenvalues/eigenspaces of the spectrum* (36) *in $\mathbf{A}_{\mathsf{N}}^p(\Sigma)$ converge towards the corresponding continuous true Maxwell eigenpairs as $p \to \infty$.*

To conclude this section, we present in Table 4 the computed values of the *positive* eigenvalues in $\mathbf{A}_{\mathsf{N}}^p(\Sigma)$ for $p = 4$ and compare them with the characterization introduced in this section. We performed the computations on the unit square. In addition to the 23 reported values, as expected, there are 9 vanishing eigenvalues (total number of degrees of freedom is $32 = 2p^2$). Comparing to Table 1, the eigenvalues of type **(b)** are easily individuated. In order to identify the eigenvalues of type **(c)**, we report in Table 5 the computed eigenvalues of problem (56). It is immediate to recognize the four simple eigenvalues $\mu_j^+[1]$, namely they are at rank 3, 8, 20, and 23 in Table 4. Since in this case we have $\lambda_0 = 9.118906527810$ (see Table 3), we still have two more eigenvalues to identify, namely the 6th and 7th. According to our theory, these are of type (d^+).

TABLE 4. Positive eigenvalues computed with ABF element in the unit square, compared with 1D eigenvalues according to Theorem 14

rank	ABF eigenvalue	type	sub-type	j	k	ρ	1D eigenvalue
1	1.000014713885	**(b)**		1		—	1.000014713885
2	1.000014713885	**(b)**				—	*idem*
3	2.000029427771	**(c)**	(s^+)	1		1	2.000029427771
4	4.002344086420	**(b)**		2		—	4.002344086420
5	4.002344086420	**(b)**				—	*idem*
6	4.923839843414	**(c)**	(d^+)	1	2	1.980850169919	4.923839843418
7	4.923839843414	**(c)**				*idem*	*idem*
8	7.323454628413	**(c)**	(s^+)	2		1	7.323454628459
9	10.34795785405	**(b)**		3		—	10.34795785405
10	10.34795785405	**(b)**				—	*idem*
11	11.34797256794	**(c)**	(d^+)	1	3	3.216800521890	11.34797256794
12	11.34797256794	**(c)**				*idem*	*idem*
13	12.70664593090	**(c)**	(d^+)	2	3	2.094556448849	12.70664593696
14	12.70664593525	**(c)**				*idem*	*idem*
15	19.10628034324	**(c)**	(s^-)	4		1	19.10628034398
16	20.31473998772	**(b)**		4		—	20.31473998774
17	20.31473998773	**(b)**				—	*idem*
18	20.39325894402	**(c)**	(d^+)	2	4	4.403743735161	20.39325894463
19	20.39325894423	**(c)**				*idem*	*idem*
20	20.69591570929	**(c)**	(s^+)	3		1	20.69591570811
21	21.95839595533	**(c)**	(d^+)	3	4	1.059246356402	21.95839599126
22	21.95839598555	**(c)**				*idem*	*idem*
23	22.20443317515	**(c)**	(s^+)	4		1	22.20443317588

TABLE 5. Eigenvalues of $A + B$ in the unit interval

rank	eigenvalue
1	2.000029428
2	7.323454628
3	20.69591571
4	22.20443317

References

1. *Handbook of mathematical functions, with formulas, graphs and mathematical tables*, Edited by Milton Abramowitz and Irene A. Stegun. Fifth printing, with corrections. National Bureau of Standards Applied Mathematics Series, Vol. 55, National Bureau of Standards, Washington, D.C., (for sale by the Superintendent of Documents, U.S. Government Printing Office, Washington, D.C., 20402), 1966.
2. D.N. Arnold, D. Boffi, and Falk R.S., *Quadrilateral H(div) finite elements*, SIAM J. Numer. Anal. (2004), to appear.
3. D. Boffi, *Fortin operator and discrete compactness for edge elements*, Numer. Math. **87** (2000), no. 2, 229–246.
4. ———, *A note on the de Rham complex and a discrete compactness property*, Appl. Math. Lett. **14** (2001), no. 1, 33–38.
5. D. Boffi, L. Demkowicz, and M. Costabel, *Discrete compactness for p and hp 2D edge finite elements*, Math. Models Methods Appl. Sci. **13** (2003), no. 11, 1673–1687.
6. D. Boffi, P. Fernandes, L. Gastaldi, and I. Perugia, *Computational models of electromagnetic resonators: analysis of edge element approximation*, SIAM J. Numer. Anal. **36** (1999), no. 4, 1264–1290.
7. D. Boffi and L. Gastaldi, *Edge finite elements for the approximation of Maxwell resolvent operator*, M2AN Math. Model. Numer. Anal. **36** (2002), no. 2, 293–305.
8. D. Boffi, J. Schöberl, and F. Kikuchi, *Edge element computation of Maxwell's eigenvalues on general quadrilateral meshes*, in preparation.
9. A. Buffa, M. Costabel, and M. Dauge, *Algebraic convergence for anisotropic edge elements in polyhedral domains*, Preprint, Pavia N. 28-PV, Istituto di Matematica Applicata e Tecnologie Informatiche CNR, 2003. *To appear* in Numer. Math.
10. A. Buffa, R. Hiptmair, T. von Petersdorff, and C. Schwab, *Boundary element methods for Maxwell transmission problems in Lipschitz domains*, Numer. Math. **95** (2003), no. 3, 459–485.
11. S. Caorsi, P. Fernandes, and M. Raffetto, *On the convergence of Galerkin finite element approximations of electromagnetic eigenproblems*, SIAM J. Numer. Anal. **38** (2000), no. 2, 580–607 (electronic).
12. M. Costabel and M. Dauge, *Singularities of electromagnetic fields in polyhedral domains*, Arch. Ration. Mech. Anal. **151** (2000), no. 3, 221–276.
13. ———, *Computation of resonance frequencies for Maxwell equations in non-smooth domains*, Topics in Computational Wave Propagation, Lect. Notes Comput. Sci. Eng., vol. 31, Springer, Berlin, 2003, pp. 125–161.
14. M. Costabel, M. Dauge, and S. Nicaise, *Singularities of Maxwell interface problems*, M2AN Math. Model. Numer. Anal. **33** (1999), no. 3, 627–649.
15. L. Demkowicz, *Fully automatic hp-adaptivity for Maxwell's equations*, Tech. Report 03-45, ICES, 2003.
16. L. Demkowicz and I. Babuška, *p interpolation error estimates for edge finite elements of variable order in two dimensions*, SIAM J. Numer. Anal. **41** (2003), no. 4, 1195–1208 (electronic).
17. L. Demkowicz and A. Buffa, *H^1, $H(curl)$ and $H(div)$-conforming projection-based interpolation in three dimensions*, Tech. Report 04-24, ICES, 2004.
18. L. Demkowicz, P. Monk, L. Vardapetyan, and W. Rachowicz, *de Rham diagram for hp finite element spaces*, Comput. Math. Appl. **39** (2000), no. 7-8, 29–38.
19. L. Demkowicz and L. Vardapetyan, *Modeling of electromagnetic absorption/scattering problems using hp-adaptive finite elements*, Comput. Methods Appl. Mech. Engrg. **152** (1998), no. 1-2, 103–124, Symposium on Advances in Computational Mechanics, Vol. 5 (Austin, TX, 1997).
20. F. Gardini, *Discrete compactness property for quadrilateral finite element spaces*, Numer. Methods Partial Differential Equations (to appear).
21. P. Grisvard, *Singularities in boundary value problems*, Recherches en Mathématiques Appliquées [Research in Applied Mathematics], vol. 22, Masson, Paris, 1992.
22. R. Hiptmair, *Finite elements in computational electromagnetism*, Acta Numer. **11** (2002), 237–339.
23. F. Kikuchi, *On a discrete compactness property for the Nédélec finite elements*, J. Fac. Sci. Univ. Tokyo Sect. IA Math. **36** (1989), no. 3, 479–490.
24. P. Monk, *On the p- and hp-extension of Nédélec's curl-conforming elements*, J. Comput. Appl. Math. **53** (1994), no. 1, 117–137.

25. ———, *Finite element methods for Maxwell's equations*, Numerical Mathematics and Scientific Computation, Oxford University Press, 2003.
26. P. Monk and L. Demkowicz, *Discrete compactness and the approximation of Maxwell's equations in* $\mathbb{R}^3$, Mathematics of Computation **70** (2000), no. 234, 507–523.
27. J.-C. Nédélec, *Mixed finite elements in* $\mathbf{R}^3$, Numer. Math. **35** (1980), no. 3, 315–341.
28. ———, *A new family of mixed finite elements in* $\mathbb{R}^3$, Numer. Math. **50** (1986), no. 1, 57–81.
29. W. Rachowicz and L. Demkowicz, *An hp-adaptive finite element method for electromagnetics. part I. Data structure and constrained approximation*, Comput. Methods Appl. Mech. Engrg. **187** (2000), no. 1-2, 307–337.
30. Ch. Schwab, *p- and hp-finite element methods*, Numerical Mathematics and Scientific Computation, The Clarendon Press Oxford University Press, New York, 1998, Theory and applications in solid and fluid mechanics.

Dipartimento di Matematica "F. Casorati", Università di Pavia, I-27100 Pavia, Italy
E-mail address: boffi@dimat.unipv.it
URL: http://www-dimat.unipv.it/boffi/

IRMAR, Institut Mathématique, Université de Rennes 1, 35042 Rennes, France
E-mail address: costabel@univ-rennes1.fr
URL: http://perso.univ-rennes1.fr/martin.costabel/

IRMAR, Institut Mathématique, Université de Rennes 1, 35042 Rennes, France
E-mail address: dauge@univ-rennes1.fr
URL: http://perso.univ-rennes1.fr/monique.dauge/

The Institute for Computational Engineering and Sciences, The University of Texas at Austin, Austin, TX 78712
E-mail address: leszek@ices.utexas.edu
URL: http://www.ices.utexas.edu/~leszek/